Carbon and hydrogen isotopic compositions of stratospheric methane: 1. High-precision observations from the NASA ER-2 aircraft

A. L. Rice,[1,2] S. C. Tyler,[3] M. C. McCarthy,[4] K. A. Boering,[4,5] and E. Atlas[6]

Received 14 October 2002; revised 7 March 2003; accepted 26 March 2003; published 8 August 2003.

[1] Measurements of $\delta^{13}C$ and δD of atmospheric CH_4 from whole air samples collected in the upper troposphere and lower stratosphere aboard the NASA ER-2 aircraft during the SOLVE (2000), POLARIS (1997), and STRAT (1996) campaigns are reported. Samples cover latitudes from 1°S to 89°N and altitudes from 11 to 21 km, providing CH_4 mixing ratios that range from 1744 to 716 ppbv. Measurements of isotope ratios were made by continuous-flow gas chromatography isotope ratio mass spectrometry which provides high-precision analyses on 60 ml aliquots of air. These measurements comprise the first upper atmosphere isotopic CH_4 data set to date using this technique and the most extensive with respect to latitude and season in any case. Values of $\delta^{13}C$-CH_4 on the V-PDB scale range from −47.28‰ near the tropical tropopause to −34.05‰ in the high northern latitude stratosphere. Values of δD on the V-SMOW scale range from −90.9‰ to +26.4‰. Correlations of isotope ratios with CH_4 mixing ratios show enrichment in the heavy isotopes as CH_4 mixing ratios decrease due to kinetic isotope effects associated with oxidation by reaction with OH, Cl, and $O(^1D)$. Empirical fractionation factors are found to be highly dependent on the range of CH_4 mixing ratio considered, increasing with decreasing mixing ratio. Systematic nonlinearity in a Rayleigh fractionation model suggests a range of stratospheric fractionation factors, $\alpha^C_{strat} = 1.0108 \pm 0.0004$ to 1.0204 ± 0.0004 (2σ) and $\alpha^H_{strat} = 1.115 \pm 0.008$ to 1.198 ± 0.008 (2σ), from high to low CH_4 mixing ratio, respectively. The variation in α over the range in mixing ratios reflect changes in partitioning between CH_4 sink reactions in different regions of the stratosphere. In Part 1, these new high-precision observations are discussed and compared with other stratospheric and tropospheric isotope measurements. In Part 2 [*McCarthy et al.*, 2003] the observations are compared with 2-D model results, and implications for the kinetic isotope effects for reactions with OH, Cl, and $O(^1D)$ are discussed. *INDEX TERMS:* 0340 Atmospheric Composition and Structure: Middle atmosphere—composition and chemistry; 0341 Atmospheric Composition and Structure: Middle atmosphere—constituent transport and chemistry (3334); 1040 Geochemistry: Isotopic composition/chemistry; 1610 Global Change: Atmosphere (0315, 0325); *KEYWORDS:* methane, stratospheric methane, methane isotopes, carbon isotopes, hydrogen isotopes

Citation: Rice, A. L., S. C. Tyler, M. C. McCarthy, K. A. Boering, and E. Atlas, Carbon and hydrogen isotopic compositions of stratospheric methane: 1. High-precision observations from the NASA ER-2 aircraft, *J. Geophys. Res.*, *108*(D15), 4460, doi:10.1029/2002JD003042, 2003.

1. Introduction

[2] Methane (CH_4) is the most abundant reactive trace gas in the Earth's atmosphere. Considerable research since the 1970s has established its role in both climate [*Donner and Ramanathan*, 1980; *Ramanathan et al.*, 1985; *Dickinson and Cicerone*, 1986] and atmospheric chemistry [*Levy*, 1971; *Thompson and Cicerone*, 1986; *Crutzen*, 1987]. As a radiatively active gas, increases in CH_4 due to anthropogenic activities are responsible for roughly 20% of the increase in direct radiative forcing since the industrial revolution [*Shine et al.*, 1996]. Relative to CO_2, its global warming potential is 62 based on a 20 year time horizon [*Ramaswamy et al.*, 2001]. As a reactive trace species, its oxidation in the atmosphere ultimately affects hydroxyl radical, ozone, and carbon monoxide levels in the troposphere and chlorine, ozone, and water vapor levels in the stratosphere.

[1]Department of Chemistry, University of California, Irvine, California, USA.
[2]Now at Joint Institute for the Study of the Atmosphere and Ocean, University of Washington, Seattle, Washington, USA.
[3]Department of Earth System Science, University of California, Irvine, California, USA.
[4]Department of Chemistry, University of California, Berkeley, California, USA.
[5]Department of Earth and Planetary Science, University of California, Berkeley, and Earth Science Division, Lawrence Berkeley National Laboratory, Berkeley, California, USA.
[6]Atmospheric Chemistry Division, National Center for Atmospheric Research, Boulder, Colorado, USA.

0148-0227/03/2002JD003042$09.00

[3] Methane from air bubbles trapped in firn and ice from Greenland and Antarctica [*Robbins et al.*, 1973; *Craig and Chou*, 1982; *Rasmussen and Khalil*, 1984; *Etheridge et al.*, 1992, 1998] indicate that CH_4 in the atmosphere has more than doubled in concentration in the last 200 years. Systematic measurements of CH_4 mixing ratio in the troposphere beginning in 1978 established a CH_4 growth rate of about 1 % per year [*Steele et al.*, 1987; *Blake and Rowland*, 1988] which remained at a relatively constant rate of increase through the 1980s. Since the early 1990s, however, the growth rate has slowed overall and has shown perplexing variations including both increases and decreases over relatively short timescales [*Dlugokencky et al.*, 2001]. Neither the overall increase in atmospheric CH_4 since the industrial revolution nor the significant variations in the growth rate are quantitatively and mechanistically understood. The lack of understanding of CH_4 changes in the past makes future forecasting difficult.

[4] *Stevens and Rust* [1982] proposed that a mass-weighted stable carbon isotopic balance between CH_4 sources and sinks combined with measurements of the $^{13}C/^{12}C$ ratio in atmospheric CH_4 would help constrain the global CH_4 budget. As a general rule, characteristic isotope ratios for individual CH_4 sources occur due to fractionation effects such as diffusion processes in which isotopic versions of the same compound are separated by mass, and kinetic processes in which chemical reactions requiring an activation energy take place at different rates depending on the isotopic substitution [e.g., *Hoefs*, 1987]. Stevens and Rust reasoned that in steady state, the weighted sum of isotope signatures from all sources should equal the well-mixed atmospheric value after adjusting for isotope fractionation effects by sink processes. Subsequent studies have shown that both C and H isotopically-weighted atmospheric CH_4 budgets are indeed useful, but are complicated by seasonal cycles in CH_4 sources and sink processes as well as overlap in isotopic signatures in CH_4 sources and uncertainty in kinetic isotope effects (KIEs) in CH_4 loss processes [e.g., *Cantrell et al.*, 1990; *Gupta et al.*, 1996].

[5] Despite a growing number of atmospheric CH_4 isotopic measurements [e.g., *Tyler et al.*, 1999; *Quay et al.*, 1999; *Lowe et al.*, 1999; *Bergamaschi et al.*, 2000], lengthy analyses associated with sample collection, vacuum line preparation, and dual inlet isotope ratio mass spectrometry (IRMS) measurement have so far limited the usefulness of stable isotopic CH_4 data in quantifying CH_4 source magnitudes and their spatial distributions to within the needed uncertainties. This limitation is particularly true of the upper troposphere and stratosphere where sampling large volumes of air is difficult. To date, there are only a handful of high precision data from these regions of the atmosphere [*Wahlen et al.*, 1989; *Brenninkmeijer et al.*, 1995; *Sugawara et al.*, 1997; *Tyler et al.*, 1999]. Several recent modeling studies have noted that the dearth of stratospheric isotopic data, in particular, has limited the ability of the models to evaluate CH_4 source strengths and distributions, the seasonality of CH_4 source functions, and experimentally determined KIEs in CH_4 sink processes [*Gupta et al.*, 1996; *Bergamaschi et al.*, 1996; *Tyler et al.*, 1999; *McCarthy et al.*, 2001; *Saueressig et al.*, 2001; *Wang et al.*, 2002]. Additional stratospheric isotopic CH_4 observations will promote a better understanding of stratospheric CH_4 isotope fractionation, which, in turn, will provide tighter constraints on the influence of stratospheric photochemistry on free tropospheric isotope values. Current models predict stratospheric enrichment of tropospheric $\delta^{13}C$-CH_4 to be 0.2 to 1.0 ‰ [*Gupta et al.*, 1996; *McCarthy et al.*, 2001; *Wang et al.*, 2002]. By convention, measurements of $^{13}C/^{12}C$ ratios are expressed relative to Pee Dee Belemnite (V-PDB) carbonate, as established by the International Atomic Energy Agency (IAEA) in Vienna, Austria, using δ notation (parts per thousand or "per mil") [*Craig*, 1957]: $\delta^{13}C = [(^{13}C/^{12}C)_{sam}/(^{13}C/^{12}C)_{std} - 1] \times 1000$. Similarly, measurements of D/H ratios in atmospheric CH_4 are expressed in the δ notation and reported relative to Standard Mean Ocean Water (V-SMOW) as established by the IAEA [*Coplen*, 1995; *Gonfiantini et al.*, 1995].

[6] In this study, we report an extensive new set of high precision measurements of the $\delta^{13}C$ and δD values of stratospheric and upper tropospheric CH_4 made possible through the recent development of an online CH_4 preconcentration system coupled to a continuous-flow gas chromatograph isotope ratio mass spectrometer (cf-GC/IRMS). The cf-IRMS system requires roughly three orders of magnitude less volume of whole air at ambient CH_4 concentration and significantly less preparation time than analysis by conventional dual inlet mass spectrometry with prior off-line air sample preparation [*Rice et al.*, 2001]. Isotope analyses of small aliquots ($\sim$60 ml) of whole air from 78 samples collected aboard the NASA ER-2 aircraft between December 1996 and March 2000 from 1°S to 89°N at altitudes from 11 to 21 km were performed. In Part 1 experimental methods and observations will be presented, following which the application and limitations of a chemistry-only fractionation model to interpretation of CH_4 oxidation will be discussed. In addition, the effects of transport on observed isotope:tracer relationships will be evaluated. Finally, a comparison to previous stratospheric and tropospheric measurements is presented. In Part 2 [*McCarthy et al.*, 2003], the observations are compared to 2-D model results and their use as diagnostics for model transport and chemistry are explored. Implications of these new measurements and model results for KIEs in the reactions of CH_4 with OH, Cl, and $O(^1D)$ are discussed.

2. Experimental Methods

2.1. Sample Collection and Storage

[7] Whole air samples were collected for both trace gas mixing ratio and isotopic analyses from the NASA ER-2 aircraft using the National Center for Atmospheric Research Whole Air Sampler (NCAR WAS) instrument during three NASA campaigns—the last deployment of the Stratospheric Tracers of Atmospheric Transport (STRAT) mission in December 1996 [e.g., *Andrews et al.*, 2001b], the Photochemistry of Ozone Loss in the Arctic Region in Summer (POLARIS) mission from April to September 1997 [*Newman et al.*, 1999], and the Stratospheric Aerosol and Gas Experiment (SAGE) III Ozone Loss and Validation Experiment (SOLVE) mission from January to March 2000 [*Newman et al.*, 2002]. The deployments allowed for substantial sampling in the tropics and midlatitudes as well as in the Arctic vortex at the end of the winter of 1997 and during the winter of 2000, both years which showed record Arctic ozone losses due to the related factors of unusually

cold temperatures and the persistence of the vortex [e.g., *Coy et al.*, 1997; *Richard et al.*, 2001]. The sampling periods also cover the chemical and dynamical evolution of the Arctic region in summer from April through mid-September in 1997 [*Newman et al.*, 1999]. Although the maximum altitude of the ER-2 aircraft is less than 22 km when fully-instrumented, in situ measurements of CO_2 and SF_6 measurements indicate that air that had descended from much higher altitudes (with mean ages as old as 6.5 years and N_2O values as low as 50 ppbv, implying descent from altitudes > 35 km) were frequently sampled [e.g., *Andrews et al.*, 2001b]. These samples therefore provide information on isotope fractionation occurring far above the ER-2 ceiling. Moreover, the numerous in situ measurements of both long-lived and short-lived compounds and meteorological parameters that were made on these flights [e.g., *Newman et al.*, 1999] provide important insight into the chemical and dynamical context of the sampled air that would be more difficult to discern for data collected by a whole air sampler flying alone.

[8] The WAS instrument flew in the right, left or "belly" pods of the ER-2 depending on deployment. The instrument itself consists of 29 to 49 electropolished 1.6-liter stainless steel canisters, a 4-stage metal bellows pump, a stainless steel manifold, electric valve actuators, and an electronics package for valve and pump control [*Flocke et al.*, 1999]. The metal bellows pump pressurizes the instrument manifold to ~3000 hPa (40 psia), which results in a collection time of 10 to 200 seconds depending on altitude and a sample volume of ~4.5 standard liters. After sample collection, the canisters were shipped to NCAR for measurement of trace gas mixing ratios by GC (see below). After GC analysis, the canisters contained ~ 2 to 4 standard liters of air and were shipped to the University of California at Berkeley for archival storage. Approximately half of each remaining sample was transferred on a vacuum line to an evacuated (10^{-5} hPa) archival 1.5 liter Pyrex flask with a Loeuwers-Hapert glass valve and Viton o-rings for measurements of $\delta^{13}C$ and δD of CH_4, δD of H_2, $\delta^{18}O$ and bulk and site-specific $\delta^{15}N$ of N_2O, and $\delta^{15}N$ of N_2 while the remaining half was reserved for measurements of $\delta^{17}O$ and $\delta^{18}O$ of CO_2. To insure that substantial isotopic fractionation had not occurred during sample collection and storage, 37 samples were analyzed by Michael Bender of Princeton University for $^{15}N/^{14}N$ ratios in N_2 since shifts in the isotopic composition of N_2 relative to its known constant value in the atmosphere would indicate significant mass fractionation of the whole air samples at some point in the collection and storage history. The Princeton analyses indicate that an upper limit to such fractionation for $\delta^{13}C$-CH_4 and δD-CH_4 is < 0.1‰. This upper limit provided by the $\delta^{15}N$ of N_2 measurements is on the order of the measurement precision for $\delta^{13}C$-CH_4 and better than that for δD-CH_4 (see below).

2.2. Measurements of CH_4 Mixing Ratio and Meteorological Parameters

[9] Mixing ratios of CH_4 were measured using a Hewlett Packard model 5890 gas chromatograph (Agilent, formerly Hewlett-Packard, San Jose, CA) fitted with a flame ionization detector (GC-FID). Calibration is based on the National Institute Standards and Technology (NIST) scale using NIST standards of 913 ± 10 ppbv and 1190 ± 10 ppbv. Precision of measurement is better than 10 ppbv (1σ). Accuracy is better than ±20 ppbv (1σ).

[10] In situ measurements of temperature, pressure, and position were made by the ER-2 Meteorological Measurement System (MMS) [*Scott et al.*, 1990]. Pressure altitude and potential temperature (θ) are derived from the temperature and pressure measurements, and all data are reported for each flight at 1-second time intervals. An average of these variables over the WAS canister filling times are used to determine the latitude, longitude, pressure altitude, and potential temperature for each WAS sample as reported below. Finally, the Microwave Temperature Profiler [*Denning et al.*, 1989] made measurements of the vertical temperature profile both above and below the aircraft and reported the altitude and potential temperature of the tropopause every 10 seconds along the flight track. From these data, samples collected in the upper troposphere, lowermost stratosphere ($\theta < 380$K), and "overworld" ($\theta \geq 380$K) can be distinguished.

2.3. Measurements of Isotope Ratios in CH_4

[11] Isotopic measurements of D/H and $^{13}C/^{12}C$ in CH_4 were made using continuous-flow gas chromatography isotope ratio mass spectrometry at the University of California, Irvine [*Rice et al.*, 2001]. Prior to isotopic analyses, pressure in the 1.5-L flasks ranged from ~500 to 1150 torr. Aliquots for isotopic analysis of the whole air samples were taken by equilibrating sample flasks with an evacuated (10^{-3} mbar) 60 ml double-valved Pyrex sample bulb using a small volume gas transfer vacuum line. In all, 78 samples were measured for $^{13}C/^{12}C$ and 76 samples for D/H ratios in atmospheric CH_4, with separate aliquots required for the C and H isotope determinations. Two fewer samples were analyzed for D/H content due to a lack of sufficient pressure in two flasks to remain in linear range for D/H measurement. In several cases multiple aliquots of a given flask were taken for measurement of either C or H isotopes in order to perform replicate analyses for determination of precision over the concentration range of samples analyzed. From the larger set of whole air samples archived at UC Berkeley (~400), samples were chosen to span the widest range of CH_4 mixing ratios and latitudes possible.

[12] A schematic of the analytical system is shown in Figure 1. Full description of isotopic analysis is described in *Rice et al.* [2001]. Briefly the 60 ml aliquot of ambient air is introduced for measurement through a system consisting of 3 traps designed to preconcentrate CH_4 and remove gases that interfere with analysis (e.g., N_2, O_2, Ar, CO_2, H_2O, NMHCs). A PoraPLOT Q (Chrompack, Raritan, NJ) separation column allows further separation of CH_4 from residual gas components in the cryofocused sample. The capillary separation column is temperature-, flow-, and pressure-regulated by a HP 6890 GC with electronic pressure control. As CH_4 elutes from the separation column it is either quantitatively oxidized to CO_2 and H_2O for carbon analysis in a combustion furnace in an alumina tube packed with CuO, NiO, and Pt wires at 960°C, or quantitatively pyrolyzed to H_2 and C for hydrogen analysis in an open alumina tube at 1450°C. Subsequently, the H_2 or CO_2 sample is swept through a Nafion dryer (Permapure Inc., Toms River, NJ) with a counter current of ultra-high purity (UHP) He to remove H_2O entrained in carrier flow as a

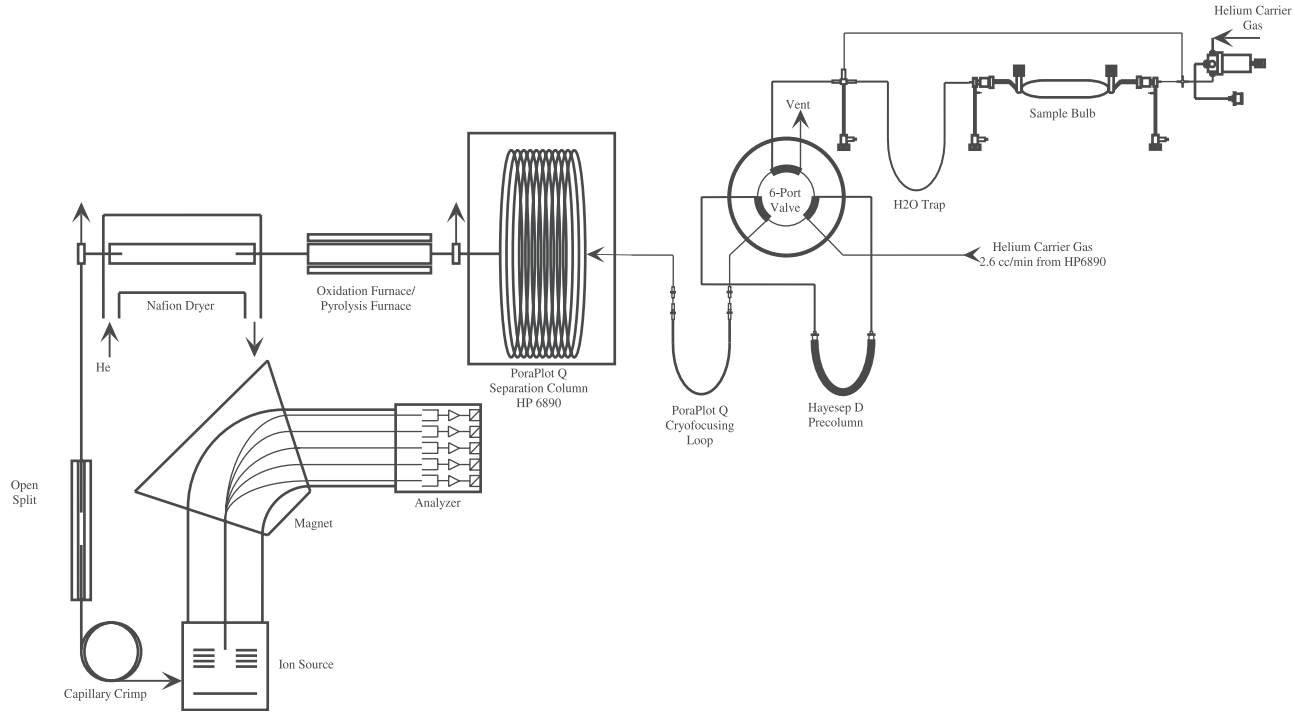

Figure 1. Schematic view of continuous-flow preconcentration gas chromatograph isotope ratio mass spectrometer system for measurement of $\delta^{13}C$ and δD of atmospheric CH_4. Reproduced with permission from *Rice et al.* [2001]. Copyright 2001 by the American Chemical Society.

result of CH_4 combustion or column bleed. Samples are introduced into the IRMS via a ThermoQuest/Finnigan (Bremen, Germany) Combustion III open split interface, a capillary leak leading directly to the ion source.

[13] Measurements of isotope ratio are made on a 3-kV ThermoQuest/Finnigan MAT Delta Plus XL IRMS relative to bracketed reference peaks admitted directly to the ion source in a balance of He carrier via a second open split. Isotopic composition of CH_4 in the whole air samples was measured versus working reference gas cylinders of UHP CO_2 and H_2 (Oxygen Services Co., Costa Mesa, CA). These reference gases were calibrated using a dual inlet IRMS (Finnigan MAT model 252) with isotope reference gases obtained from the National Institute of Water and Atmospheric Research (NIWA, Wellington, New Zealand) and Oztech Gas Company (Dallas, TX) [*Rice et al.*, 2001; *Tyler et al.*, 1999]. Dual inlet CO_2 working gas standards are routinely compared with two internationally recognized CO_2 standards, NBS-19 ($CaCO_3$) and IAEA-CO-9 ($BaCO_3$) which have established values of 1.95 and −47.12‰, respectively [*Stichler*, 1995]. Versus our −47.61‰ primary CO_2 working reference gas (designated NZME, from NIWA), clean dry CO_2 gas standards made from these carbonates have measured values of 1.92 and −47.18‰ for NBS-19 and IAEA-CO-9, respectively. Dual inlet H_2 reference gases are a suite of three calibrated standards from Oztech with values of −108.0, −165.3, and −306.8‰ with respect to V-SMOW and are intercompared regularly with a precision of ±1.0‰. Values for the Delta Plus IRMS reference gas cylinders are −34.28 ± 0.01‰ (1σ, n = 5) $\delta^{13}C$-CO_2 relative to V-PDB and −169.4 ± 0.5‰ (1σ, n = 5) δD-H_2 relative to V-SMOW.

[14] To insure long-term system stability and measurement integrity, a calibrated whole air tank was measured at least twice on each date sample measurements were made throughout the several week ER-2 sample analysis period. Measurements of this whole air sample during isotopic analysis averaged −47.12 ± 0.06‰ (n = 18, 1σ) for $\delta^{13}C$-CH_4 and −84.6 ± 1.6‰ (n = 23, 1σ) for δD-CH_4 with no discernable trend in either $\delta^{13}C$ or δD over measurement periods. Calibrations for $\delta^{13}C$ and δD of atmospheric CH_4 are described in *Rice et al.* [2001].

[15] Precision of measurement for both $\delta^{13}C$-CH_4 and δD-CH_4 was also evaluated by running replicates of selected samples, as noted above, which convolves the precision of both sample transfer and isotopic analysis and provides an indication of precision on samples that had CH_4 concentrations significantly lower than the tropospheric average (∼1.75 ppmv in 1999 [*Dlugokencky et al.*, 2001]) for which the technique was originally developed. Replicates were selected so that they spanned the concentration range of ER-2 samples analyzed. Six replicates were performed for both $\delta^{13}C$-CH_4 and δD-CH_4. Using a pooled variance estimate, average precision was determined to be ±0.04 ‰ (1σ) for $\delta^{13}C$-CH_4 and ±1.25‰ (1σ) for δD-CH_4, consistent with variability observed in the calibrated whole air sample over the multiweek measurement period (±0.06‰, ±1.6‰). In neither case did precision decrease as the CH_4 mixing ratio in the samples decreased.

3. Results

[16] Measured values of $\delta^{13}C$-CH_4 for 78 whole air samples and δD-CH_4 for 76 whole air samples appear in

Table 1 along with the sample collection parameters (flight date, collection time, pressure-altitude, latitude, and longitude) and corresponding values for CH_4 mixing ratio. Also indicated in Table 1 are the 3 samples that were collected below the local tropopause (as measured by the Microwave Temperature Profiler) and the samples that were collected in the Arctic vortex (as indicated by PV analyses for POLARIS [*Coy et al.*, 1997; *Newman et al.*, 1999] or N_2O:potential temperature analyses for SOLVE [*Greenblatt et al.*, 2002]).

[17] Figure 2 illustrates both the extensive coverage in the Northern Hemispheric lower stratosphere and the general trend in CH_4 mixing ratio and isotopic composition with respect to latitude and altitude as contours of CH_4 mixing ratio (Figure 2a), $\delta^{13}C$-CH_4 (Figure 2b), and δD-CH_4 (Figure 2c). Contour lines were generated by MATLAB (version 5.3, The MathWorks, Inc., Natick, MA). Samples ranged in CH_4 mixing ratio between 1744 ppbv in a sample from the upper troposphere down to 716 ppbv in the polar vortex. Within this range of mixing ratios, corresponding isotope values ranged from −47.28‰ to −34.05‰ for $\delta^{13}C$-CH_4. The four lightest values (−47.28‰, −47.23‰, −47.23‰, and −47.21‰) were measured on samples collected in the midlatitude lowermost stratosphere (1 sample) and the high latitude (2 samples) and tropical upper troposphere (1 sample). These values fall within the range of Northern Hemispheric free troposphere reported by *Tyler et al.* [1999] from two Northern Hemisphere land based tropospheric clean air collection sites (∼−46.8 to −47.6‰). In a similar manner, values of $\delta D-CH_4$ range from −90.9‰ in an upper tropospheric sample to +26.4‰ in the polar vortex. Observations in the tropical, midlatitude, and high latitude upper troposphere of −84.7‰, −87.6‰, and −87.4‰ fall within the range of values reported previously by *Quay et al.* [1999] for the remote Northern Hemisphere troposphere (∼−75 to −105‰). For both $\delta^{13}C$-CH_4 and δD-CH_4, observations from within the polar vortex are among the most isotopically enriched high-precision measurements ever to be reported for atmospheric CH_4.

[18] Although Figure 2 graphically illustrates the general trend of decreasing CH_4 and increasingly enriched carbon and hydrogen isotopic compositions as altitude and latitude increase, these 78 samples were collected over four years during different seasons. Due to (1) the small number of samples, (2) known seasonal variations in CH_4 mixing ratios as a function of latitude and altitude [e.g., *Michelsen et al.*, 1998], and (3) the fact that high spatial resolution aircraft measurements can resolve the existence of narrow filaments of air representative of a different region (e.g., polar or tropical filaments encountered during midlatitude flights [e.g., *Boering et al.*, 1996; *Herman et al.*, 1998]), the contours in Figure 2 should be considered a qualitative representation of the observed isotopic compositions only. Details of the contour shapes are not meaningful. An alternative way of presenting the data is to plot $\delta^{13}C$-CH_4 and δD-CH_4 versus CH_4 mixing ratio (Figures 3a and 3b, respectively). Isotope:tracer plots provide a means with which to interpret CH_4 isotopic composition in terms of the effects of underlying chemistry and transport and allow variations in isotopic composition with respect to season, year, and latitude to be more easily discerned than the 2-D plots of Figure 2.

[19] Measurements of $\delta^{13}C$-CH_4 and δD-CH_4 are grouped by latitude and aircraft campaign and plotted against CH_4 mixing ratio in Figures 3a and 3b, respectively. Both the $\delta^{13}C$-CH_4:CH_4 mixing ratio relationship and the δD-CH_4:CH_4 mixing ratio relationship exhibit the same general trend; CH_4 is isotopically fractionated as it is oxidized by reaction with OH, Cl, and $O(^1D)$, becoming increasingly enriched in the heavy isotopomers ($^{13}CH_4$ and CH_3D) as CH_4 mixing ratio decreases. The change in CH_4 isotopic composition can be explained by KIEs associated with these CH_4 chemical sink reactions. For each reaction, ^{13}C and D substituted species react more slowly (i.e., have smaller rate coefficients) than the isotopically unsubstituted species. Recent experimental determinations of these KIEs are listed in Table 2 for $^{13}C/^{12}C$ (k_{12C}/k_{13C}) and Table 3 for D/H (k_H/k_D), respectively. Included are temperature dependences (if any) and values at 225K determined from the temperature dependences for point of reference. In the stratosphere, these oxidative channels combine to produce weighted kinetic isotope effects influencing the isotopic CH_4 composition, but are not expected to remain in constant ratio, however, and vary with latitude, altitude, and season in the stratosphere [*Wang et al.*, 2002; *McCarthy et al.*, 2003].

[20] Methane isotope:mixing ratio plots (Figure 3) provide compact correlations; root mean squared variability relative to a polynomial fit is 0.5‰ and 6‰ (2σ) for $\delta^{13}C$-CH_4 and δD-CH_4 respectively. Despite this generally tight correlation, however, the high latitude POLARIS data for CH_4 < 1000 ppb have a statistically significant (95% confidence interval) more depleted isotopic composition than the SOLVE data over the same range of CH_4 mixing ratios (Note that the 805 ppb CH_4 sample from POLARIS flight 970630 could not be run for δD-CH_4, however, since too little sample remained, as noted earlier). In addition, a small but discernable difference in the $\delta^{13}C$-CH_4:CH_4 mixing ratio relationship between the deep tropics and the extratropics can be seen in Figure 4 in which the data are plotted on a higher resolution scale for high CH_4 mixing ratios and binned to differentiate the deep tropics (<10°N) from the extratropics (>30°N); $\delta^{13}C$-CH_4 values are slightly enriched in the deep tropics for a given CH_4 mixing ratio compared with the extratropics. The significance of the differences in these relationships as a function of deployment and latitude are discussed in the following section.

4. Discussion

[21] As expected, and consistent with previous sets of high-precision observations [*Wahlen et al.*, 1989; *Brenninkmeijer et al.*, 1995; *Sugawara et al.*, 1997], the ER-2 observations show that CH_4 becomes enriched in heavy isotopes as CH_4 mixing ratios decrease due to kinetic isotope effects associated with the CH_4 sink reactions—that is, the isotopically unsubstituted species react more quickly with OH, Cl, and $O(^1D)$ than the ^{13}C- and D-substituted species so that the remaining CH_4 is enriched in ^{13}C and D. The new ER-2 observations extend to lower CH_4 mixing ratios than previously observed, and they span a wide range of latitudes, altitudes, years and seasons, giving a much broader picture of methane isotope fractionation than has been available in the past. A starting point of analyses of

Table 1. Whole Air Samples Collected Aboard the NASA ER-2 Analyzed for $^{13}C/^{12}C$ and D/H Ratios in Atmospheric CH_4

Flight Date, m/d/y	Collection Time, Universal, s	Pressure-Altitude, km	Latitude, °N	Longitude, °W	$[CH_4]$, ppbv	$\delta^{13}C$-CH_4, ‰ V-PDB	δD-CH_4, ‰ V-SMOW	Potential Temperature, K	Note
				STRAT					
12/9/96	86244	20.47	19.96	−158.10	1705	−47.16	−87.6	385	
12/9/96	87401	20.15	19.09	−157.59	1399	−44.80	−66.6	459	
12/9/96	87791	19.89	19.62	−157.75	1372	−44.52	−63.7	472	
12/9/96	88170	17.10	20.16	−158.18	1326	−44.14	−65.0	483	
12/11/96	84198	20.16	−1.11	−155.55	1678	−46.72	−87.0	420	
12/11/96	84922	20.05	−0.09	−155.33	1718	−47.21	−84.7	361	troposphere
12/11/96	85487	19.70	0.85	−155.36	1683	−46.90	−86.5	405	
12/11/96	87305	18.51	4.07	−155.44	1658	−46.59	−89.8	455	
12/11/96	89091	18.25	7.23	−155.47	1604	−46.26	−87.0	459	
12/11/96	91193	15.74	11.08	−155.47	1534	−45.95	−79.1	470	
12/13/96	71912	19.35	27.89	−145.95	1518	−45.88	−78.4	464	
12/13/96	72860	17.51	28.85	−144.04	1638	−46.71	−85.5	420	
12/13/96	73094	16.73	29.08	−143.55	1691	−47.12	−88.3	397	
12/16/96	72049	15.74	58.46	−117.40	1553	−45.98	−81.2	425	
12/18/96	80778	20.21	46.35	−127.41	1378	−44.56	−63.5	480	
				POLARIS I					
4/24/97	65523	20.47	42.56	−127.79	1392	−44.92	−62.0	486	
4/24/97	71551	20.00	50.25	−140.30	1548	−46.31	−80.0	441	
4/24/97	74472	16.98	55.85	−142.07	1368	−44.48	−60.3	519	
4/26/97	63362	19.14	72.23	−148.01	1129	−41.83	−43.7	502	
4/26/97	66687	19.58	79.03	−148.00	1468	−45.42	−74.9	506	
4/26/97	68367	18.99	82.51	−148.00	1308	−44.03	−60.0	505	
4/26/97	70058	19.17	86.12	−147.97	1018	−40.18	−32.4	502	vortex edge
4/26/97	71287	17.74	88.73	−147.52	882	−38.18	−11.3	501	vortex edge
4/26/97	72695	18.36	88.95	−136.27	1319	−43.96	−61.6	421	vortex
4/26/97	72913	19.13	88.56	−140.68	1526	−46.24	−79.6	397	vortex
4/26/97	73593	19.17	87.40	−145.84	1063	−41.03	−31.3	463	vortex
4/26/97	73877	15.63	86.97	−146.63	1068	−41.48	−31.4	479	vortex edge
4/26/97	74365	19.21	86.14	−147.53	1007	−40.42		498	vortex edge
4/26/97	75270	14.38	84.53	−148.00	996	−40.03	−25.7	513	
5/6/97	76553	19.36	74.24	−105.60	1269	−43.66	−55.6	513	
5/6/97	81046	20.18	71.24	−126.51	1292	−44.08	−55.7	527	
5/9/97	18283	19.42	64.41	−156.40	1363	−44.60	−60.6	498	
5/9/97	25943	19.17	64.52	−153.24	1336	−44.22	−61.7	505	
5/11/97	73375	15.71	64.02	−144.40	1653	−47.00	−84.6	330	
5/11/97	76707	13.70	62.29	−148.79	1744	−47.23	−87.6	321	troposphere
5/11/97	82306	11.26	62.94	−147.15	1606	−46.68	−81.4	388	
5/11/97	83455	9.23	64.17	−144.76	1600	−46.46	−82.7	424	
5/11/97	88383	8.65	64.27	−145.63	1633	−46.87	−83.2	357	
5/13/97	77627	17.40	84.57	−113.85	1404	−45.05	−66.7	470	
				POLARIS II					
6/26/97	72651	18.55	75.49	−147.69	1245	−43.49	−58.1	488	
6/27/97	74272	16.36	75.93	−147.65	1401	−44.84	−72.5	441	
6/29/97	89540	20.82	60.38	−137.61	884	−38.60	−23.0	527	vx. filament
6/30/97	78459	20.59	63.66	−147.85	1631	−46.72	−85.4	394	
6/30/97	81592	18.61	66.48	−147.87	1501	−45.74	−82.8	480	
6/30/97	84645	14.47	64.12	−147.85	803	−37.64		524	vx. filament
				SOLVE					
1/6/00	85004	18.40	21.53	−120.00	1672	−47.08	−80.9	435	
1/11/00	60753	11.40	43.48	−71.67	1726	−47.28	−87.4	358	
1/27/00	44072	20.25	54.95	34.14	1622	−46.47	−80.0	417	
1/27/00	47949	16.95	61.39	27.87	985	−39.81	−22.8	453	vortex
1/27/00	52761	11.69	67.04	21.82	1681	−47.00	−83.1	334	vortex
1/31/00	43541	17.87	77.84	13.36	1252	−43.40	−51.5	405	vortex
2/2/00	42344	20.37	65.83	63.05	1058	−40.81	−36.0	436	vortex
2/2/00	54542	19.01	76.03	14.97	1407	−44.82	−68.9	389	vortex
2/2/00	57487	16.69	70.77	18.90	914	−38.66	−13.2	451	vortex
2/3/00	72462	19.74	72.77	24.70	1475	−45.58	−77.2	376	vortex
2/3/00	73291	18.60	72.29	25.35	1366	−44.46	−62.5	391	vortex
2/3/00	75852	16.76	71.59	26.23	1158	−42.22	−43.9	420	vortex
2/3/00	77896	15.65	71.44	26.40	1057	−40.73	−30.7	439	vortex edge
2/3/00	79959	13.51	68.39	24.09	1663	−46.73	−81.0	349	
2/3/00	80211	11.35	68.27	23.27	1737	−47.23	−90.9	319	troposphere
3/5/00	46199	19.94	74.85	46.12	985	−39.99	−20.0	436	vortex
3/5/00	51907	19.52	80.48	12.90	752	−34.78	19.0	460	vortex
3/7/00	41808	19.47	80.69	50.68	888	−37.94	−11.1	444	vortex
3/7/00	44309	19.19	82.16	27.70	945	−39.09	−15.5	442	vortex
3/7/00	44892	16.49	81.13	25.71	1305	−43.94	−62.2	393	vortex

Table 1. (continued)

Flight Date, m/d/y	Collection Time, Universal, s	Pressure-Altitude, km	Latitude, °N	Longitude, °W	$[CH_4]$, ppbv	$\delta^{13}C$-CH_4, ‰ V-PDB	δD-CH_4, ‰ V-SMOW	Potential Temperature, K	Note
3/7/00	45191	15.95	80.59	25.20	1453	−45.23	−70.2	384	vortex
3/11/00	39893	20.19	59.38	−2.78	1604	−46.41	−80.3	422	
3/11/00	41761	20.11	61.97	1.87	1445	−44.93	−66.8	452	
3/11/00	49504	20.36	70.12	29.28	719	−34.22	22.7	460	vortex
3/11/00	50510	20.24	71.86	29.75	716	−34.05	26.4	461	vortex
3/11/00	51523	19.07	73.60	29.75	785	−35.91	15.7	457	vortex
3/11/00	53534	17.21	73.45	27.26	733	−34.30	18.3	463	vortex
3/12/00	50149	19.74	78.91	41.65	1099	−41.14	−34.0	421	vortex
3/12/00	50600	19.84	79.14	37.23	999	−39.73	−27.2	435	vortex
3/12/00	51647	19.64	79.44	26.83	854	−37.12	−4.7	448	vortex
3/12/00	53681	19.13	79.02	6.83	790	−35.78	12.9	454	vortex
3/12/00	54697	18.32	77.53	8.27	798	−36.00	11.0	453	vortex
3/16/00	28815	16.77	67.40	13.57	1614	−46.14	−81.2	426	

observed stable isotope compositions is to compare the observed fractionation with what would be expected from fractionation occurring in an isolated system (i.e., comparing observations with the Rayleigh fractionation equation). This provides a method to investigate the relative importance of CH_4 oxidative channels and a means by which to compare data sets. For illustrative purposes, we first derive a modified Rayleigh fractionation model for CH_4 oxidation through reaction with the three stratospheric sink reactions. Second, we discuss the importance of understanding transport to interpreting general trends as well as discernable differences with respect to deployment and latitude in isotope:tracer relationships in Section 4.2. Finally, we compare the ER-2 observations with other available stratospheric and upper tropospheric CH_4 isotope observations in sections 4.3 ($\delta^{13}C$) and 4.4 (δD).

4.1. Modified Rayleigh Framework

[22] If a chemistry-only model to the relationship between isotopic CH_4 and CH_4 mixing ratio is considered, where effects of transport are ignored, rates of chemical oxidation by the stratospheric sinks OH, Cl, and $O(^1D)$ can be described for the three CH_4 isotopomers by

$$\frac{d[CH_4]}{dt} = -k_{OH}[CH_4][OH] - k_{Cl}[CH_4][Cl] - k_{O(1D)}[CH_4]\left[O\left(^1D\right)\right] \quad (1)$$

$$\frac{d[^{13}CH_4]}{dt} = -k^{13}_{OH}\left[^{13}CH_4\right][OH] - k^{13}_{Cl}\left[^{13}CH_4\right][Cl] - k^{13}_{O(1D)}\left[^{13}CH_4\right]\left[O\left(^1D\right)\right] \quad (2)$$

$$\frac{d[CH_3D]}{dt} = -k^{D}_{OH}[CH_3D][OH] - k^{D}_{Cl}[CH_3D][Cl] - k^{D}_{O(1D)}[CH_3D]\left[O\left(^1D\right)\right] \quad (3)$$

Defining f_{OH}, f_{Cl}, and $f_{O(^1D)}$ as the fraction of CH_4 oxidized by OH, Cl, and $O(^1D)$ respectively, f_{OH}, for example, can be described by

$$k^{13}_{OH}[OH] = -\frac{1}{[^{13}CH_4]}\frac{d[^{13}CH_4]}{dt} f_{OH} \quad (4)$$

Dividing through (1) by $[CH_4]$ and (2) by $[^{13}CH_4]$, and then subtracting (1) from (2), the relationship for the two stable carbon isotopomers can be rearranged to become

$$\frac{1}{[CH_4]}\frac{d[CH_4]}{dt} = \frac{1}{[^{13}CH_4]}\frac{d[^{13}CH_4]}{dt} \cdot \left[\frac{k_{OH}}{k^{13}_{OH}} f_{OH} + \frac{k_{Cl}}{k^{13}_{Cl}} f_{Cl} + \frac{k_{O(1D)}}{k^{13}_{O(1D)}} f_{O(1D)}\right] \quad (5)$$

An average fractionation factor α^{C}_{strat}, can be defined from the weighted individual KIEs in equation (5)

$$\alpha^{c}_{strat} = \frac{k_{OH}}{k^{13}_{OH}} f_{OH} + \frac{k_{Cl}}{k^{13}_{Cl}} f_{Cl} + \frac{k_{O(1D)}}{k^{13}_{O(1D)}} f_{O(1D)} \quad (6)$$

Integrating (5), in the simplest case with the assumption that α^{C}_{strat} is constant over time, latitude, altitude, and temperature in the stratosphere and substituting the expression for the $\delta^{13}C$ value, the relationship becomes

$$\ln\left[\frac{[CH_4]}{[CH_4]_0}\right] = \frac{\alpha^{c}_{strat}}{1-\alpha^{c}_{strat}} \ln\left[\frac{\delta^{13}C + 1000}{\delta^{13}C_0 + 1000}\right] \quad (7)$$

Equation (7) is a modified form of the Rayleigh fractionation equation [e.g., *Davidson et al.*, 1987] where $[CH_4]$ and $\delta^{13}C$ are values of the mixing ratio and isotope ratio at any point in this relationship and $[CH_4]_0$ and $\delta^{13}C_0$ are the initial mixing ratio and carbon isotope ratio of CH_4 entering the stratosphere. Similarly, a relationship may be developed for the average hydrogen fractionation factor (α^{H}_{strat}). Note that f_{OH}, f_{Cl}, and $f_{O(^1D)}$ are the same in either case.

[23] Within the limits of this model we can evaluate average observed stratospheric fractionation factors. Figures 5a and 5b show the fits to the data for this model for calculation of average carbon and hydrogen stratospheric fractionation factors: linear regression yields α^{C}_{strat} = 1.0154 ± 0.0008 (2σ) and α^{H}_{strat} = 1.153 ± 0.010 (2σ). Despite strong correlations (r^2 = 0.989 $\delta^{13}C$-CH_4 and r^2 = 0.986 δD-CH_4), however, there is a significant degree of curvature observed in the data when fit to this linear model, clearly evident in plots of the residuals. This curvature is consistent with empirical fractionation factors that are highly dependent on the range of mixing ratio

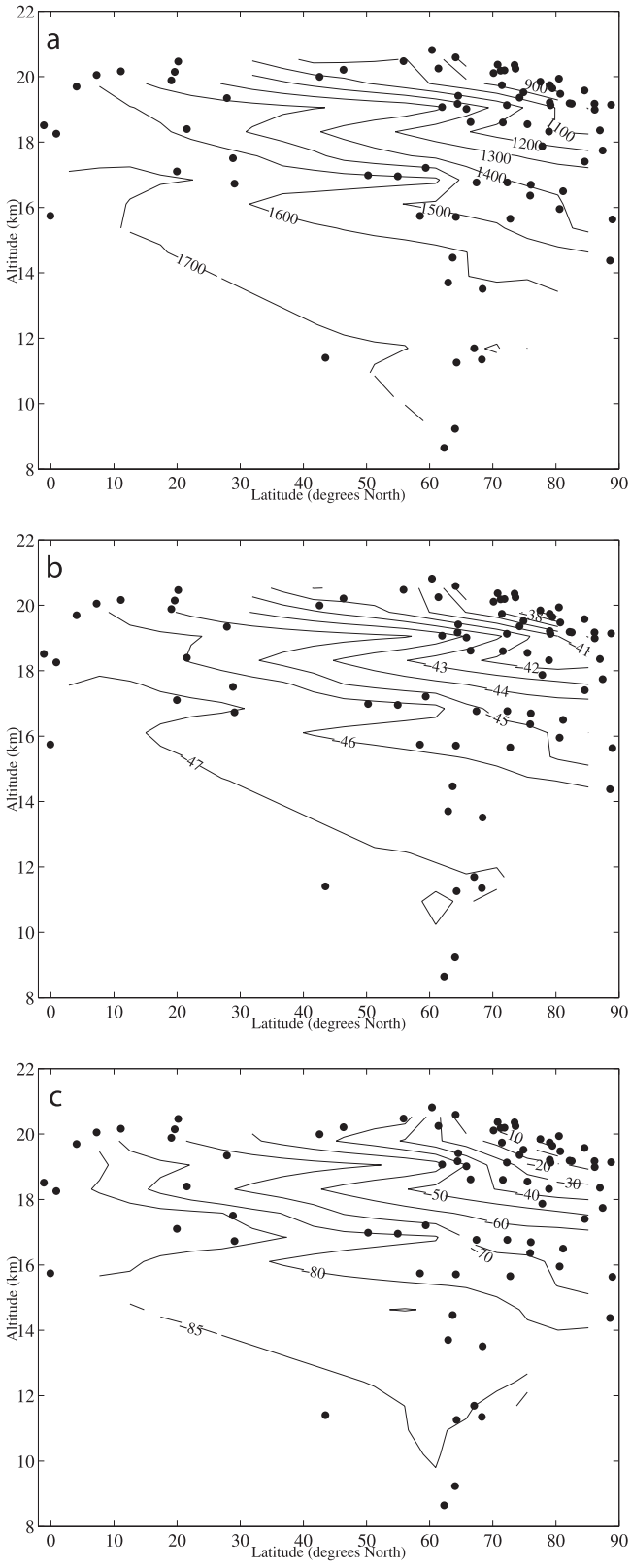

Figure 2. Altitude and latitude distribution of (a) CH_4 mixing ratio, (b) $\delta^{13}C$-CH_4, and (c) δD-CH_4 using contours generated from the STRAT, POLARIS, and SOLVE measurements by MATLAB (version 5.3, The Mathworks, Inc., Natick, MA).

considered. In fact, calculated enrichments vary roughly by a factor of two, increasing with decreasing CH_4 mixing ratio, over the entire range of observations, confirming the limitations of the Rayleigh model over a large concentration range (more than 1000 ppbv).

[24] Systematic trends in α^{C}_{strat} and α^{H}_{strat} may be empirically fit by increasing α^{C}_{strat} and α^{H}_{strat} monotonically over the range of CH_4 concentrations observed. Consider Figure 6a which shows the results of $\delta^{13}C$-CH_4 compared with true Rayleigh derived curves (dotted lines) ranging from 1.0108 ± 0.0004 to 1.0204 ± 0.0004 (2σ). Clearly no one curve adequately describes the curvature observed in the $\delta^{13}C$-CH_4:CH_4 mixing ratio relationship; different ranges are better described by differing Rayleigh curves. Data are best fit with a monotonically increasing α^{C}_{strat} with respect to CH_4 mixing ratio (solid lines) from 1.0108 at 1726 ppbv (lowermost stratospheric point) to 1.0204 at 716 ppbv (highest stratospheric point). Similarly data shown in Figure 6b for δD-CH_4 can be better described by a varying α^{H}_{strat}, from 1.115 ± 0.008 to 1.198 ± 0.008 (2σ), than by a Rayleigh relationship with a single α.

[25] This systematic nonlinearity in the Rayleigh relationship can be described in large part by changing values for f_{OH}, f_{Cl}, and $f_{O(^1D)}$ in different regions of the stratosphere. As a result, the average fractionation factor should not be expected to be constant over a large range in CH_4 mixing ratio. At higher altitudes, for example, the fraction of CH_4 oxidized by reaction with Cl and $O(^1D)$ increase (and note that this low-CH_4 air is brought back into the lower stratosphere via stratospheric circulation). The carbon KIE for reaction with Cl is $\sim$1.07 at 225 K, as compared with $\sim$1.004 to 1.005 for OH (see Table 2). Thus, as the fraction of CH_4 oxidized by Cl increases relative to OH, the average fractionation factor, α^{C}_{strat}, increases due to the much larger KIE for the reaction of CH_4 with Cl. Given the relative magnitudes of the hydrogen KIEs listed in Table 3, the 75% increase in calculated stratospheric hydrogen enrichment factors from high to low CH_4 mixing ratio is likewise best explained by an increasing importance of the chlorine oxidation channel (i.e., f_{Cl}) at lower CH_4 mixing ratios.

[26] Oxidation of CH_4 via $O(^1D)$ will also increase with altitude in the stratosphere, so that the $f_{O(^1D)}$ will increase as CH_4 mixing ratio decreases. The importance of the $O(^1D)$ oxidative channel to the concavity in the $\delta^{13}C$-CH_4:CH_4 mixing ratio relationship of Figure 3a (and hence the nonlinearity to Figure 5a), however, is highly dependent on whether the value determined from *Davidson et al.* [1987] of 1.001 or that from *Saueressig et al.* [2001] of 1.013 is considered. If $k_{c12}/k_{c13} = 1.001$, as the $O(^1D)$ consumption channel becomes increasingly important higher in the stratosphere, the role of the much larger Cl kinetic isotope effect will be diminished. Conversely, if $k_{c12}/k_{c13} = 1.013$, $O(^1D)$ oxidation will add to the curvature in Figure 3a as this channel becomes important since the magnitude of the $O(^1D)$ KIE in this case is larger than the OH KIE (although the effect will not be as dramatic as it is for the increasing importance of the Cl channel). The effect of the different $O(^1D)$ carbon KIEs on the $\delta^{13}C$-CH_4:CH_4 mixing ratio relationship is explored more quantitatively with a 2-D model in Part 2 [*McCarthy et al.*, 2003].

[27] Several additional insights into the partitioning of CH_4 oxidation in the stratosphere may be drawn from this

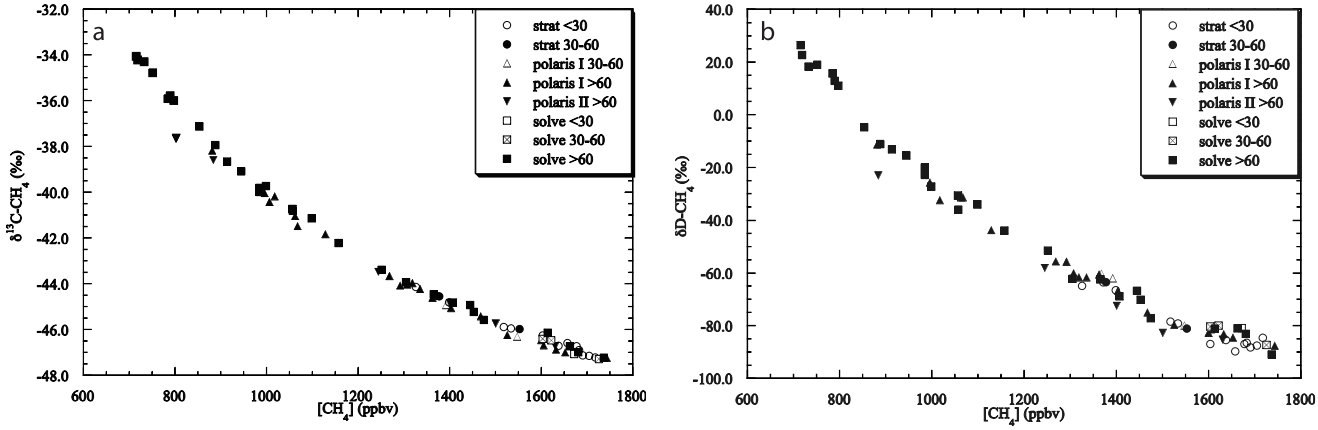

Figure 3. Correlations of (a) $\delta^{13}C$-CH_4 and (b) δD-CH_4 with CH_4 mixing ratio. Data are delineated by campaign and latitudinal bands: STRAT <30°N (open circles), STRAT 30–60°N (solid circles), POLARIS 30–60°N (open triangles), POLARIS >60°N (diamonds), POLARIS II >60°N (solid triangles), SOLVE <30°N (open squares), SOLVE 30–60°N (crosses), SOLVE >60°N (solid squares).

chemistry-only modified Rayleigh model. Noting that Cl oxidation provides the only kinetic isotope effect larger than all fractionation effects (α^{C}_{strat}) calculated in this study, there is little doubt of its overall importance to the $\delta^{13}C$-CH_4:CH_4 mixing ratio relationship and CH_4 oxidation in the stratosphere. Within the constructs of equation (7), considering measured values of kinetic isotope effects from Table 2 and assuming negligible temperature dependences of the KIEs in the stratosphere (i.e., ~180–280K), estimates of f_{Cl} may be made. Using values for the carbon KIEs of 1.0054, 1.070, and 1.001 for OH, Cl, and $O(^1D)$, respectively, the estimated lower bound for the oxidation of CH_4 by Cl is 8% for CH_4 observed at 1726 ppbv (the lower stratosphere) to 24% at 716 ppbv CH_4 (on average ~30km in the extratropics). Using values for the carbon KIEs of 1.0039, 1.073, and 1.013 decreases the estimates of both lower bounds for f_{Cl} by 3 to 4%. In this case, the decrease in the OH kinetic isotope effect is largely offset by the much larger $O(^1D)$ value. It is important to note, however, that, due to the attenuating effect that transport has on empirical fractionation factors (see section 4.2), these values for f_{Cl} generated from the chemistry-only framework (equation (7)) provide only a lower bound. Current 2-D model estimates (including transport) for the integrated effect of Cl on overall stratospheric CH_4 oxidation are 20–35% [*Gupta et al.*, 1996; *Irion et al.*, 1996; *Saueressig et al.*, 2001; *McCarthy et al.*, 2003].

[28] It is also worthwhile to compare hydrogen KIEs in Table 3 to δD-CH_4 observations within a chemistry-only framework. Empirical values of α^{H}_{strat} range from 1.115 to 1.198 and, at face value, appear to be at odds with the experimentally determined hydrogen KIEs. For example, in the lower stratosphere (at high CH_4 mixing ratios in our data set) the reaction of CH_4 with OH is expected to dominate. Using hydrogen KIEs of 1.36, 1.70, and 1.06 in equation (6) for OH, Cl, and $O(^1D)$, respectively, it is not possible to reconcile the weighted α^{H}_{strat} with observations of δD-CH_4 considering a chemistry-only model (with no transport) without an unrealistic contribution from the $O(^1D)$ reaction channel of $f_{O(^1D)} \sim 0.75$. At lower CH_4 mixing ratios stratospheric observations are more consistent with results of kinetic studies, particularly given the relatively large uncertainties associated with several of the KIE results. Considering the largest empirical fractionation factor observed from the observations of 1.198 (at 716 ppbv), this discrepancy decreases to a more realistic estimate for minimum $f_{O(^1D)}$ of 40%, a value closer to model predictions of integrated stratospheric CH_4 oxidation by $O(^1D)$ of 20–30% [*Irion et al.*, 1996; *McCarthy et al.*, 2003]. Using the

Table 2. Recent Experimental Determinations of Carbon Kinetic Isotope Effects in Stratospheric CH_4 Sink Reactions

Reaction	Study	k_{c12}/k_{c13} Temp. Dep.	k_{c12}/k_{c13} 295–298 K	k_{c12}/k_{c13} 225 K
CH_4 + OH	*Saueressig et al.* [2001]		1.0039	
	Cantrell et al. [1990]	T independent 273–353 K	1.0054	1.0054
CH_4 + Cl	*Tyler et al.* [2000]	1.035exp(7.55/T) 223–349 K	1.0621	1.070
	Crowley et al. [1999]		1.066	
	Saueressig et al. [1995]	1.043exp(6.455/T) 223–297 K	1.066	1.073
CH_4 + $O(^1D)$	*Saueressig et al.* [2001]	T independent 223–295 K	1.013	1.013
	Davidson et al. [1987]		1.001	

Table 3. Recent Experimental Determinations of Hydrogen Kinetic Isotope Effects in Stratospheric CH_4 Sink Reactions

Reaction	Study	k_H/k_D Temp. Dep.	k_H/k_D 295–298 K	k_H/k_D 225 K
CH_4 + OH	*Saueressig et al.* [2001]		1.294	
	Gierczak et al. [1997]	1.09exp(49/T) 249–422 K	1.25	1.36
	DeMore [1993]	0.91exp(75/T) 293–361 K	1.16	1.27
CH_4 + Cl	*Boone et al.* [2001]		1.54	
	Tyler et al. [2000]	0.894exp(145/T) 273–349 K	1.474	1.70
	Saueressig et al. [1996]	1.278exp(51.31/T) 223–296 K	1.508	1.60
CH_4 + $O(^1D)$	*Saueressig et al.* [2001]	T independent 223–295 K	1.06	1.06

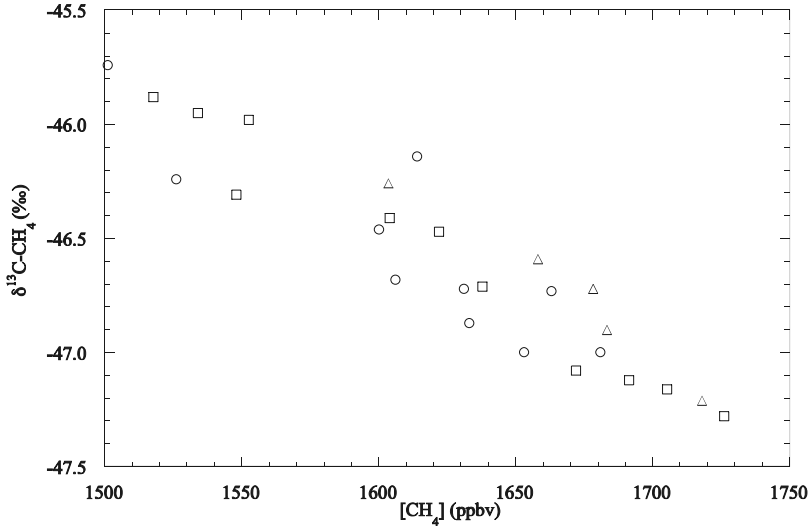

Figure 4. Higher resolution scale for the correlation of $\delta^{13}C$-CH_4 with CH_4 mixing ratio in the deep tropics <10°N (open triangles), midlatitudes 10–60 °N (open squares) and high latitudes >60 °N (open circles).

lowest values for the OH and Cl hydrogen KIEs in Table 3 and assuming a value of unity for $O(^1D)$ [*Kaye*, 1987], estimates for minimum $f_{O(^1D)}$ drop only to 50% in the lowermost stratosphere, still unrealistically high, and 14% at 716 ppbv CH_4. The apparently large discrepancy between δD-CH_4 observations and laboratory derived kinetic isotope effects can be at least partly, if not wholly, explained by the fact that stratospheric transport and mixing attenuate the isotope fractionation relative to that which is expected based on the underlying KIEs alone (see section 4.2). Although transport also affects the $\delta^{13}C$-CH_4 data, the effects on δD-CH_4 should be more pronounced due to the relative magnitude of the hydrogen KIE compared with the carbon KIE in the reaction of CH_4 with OH, particularly at higher CH_4 mixing ratios where the OH channel dominates CH_4 oxidation. In order to more realistically evaluate whether or not there is real discrepancy between the laboratory KIEs in Tables 2 and 3 and the new ER-2 isotope observations, the effects of transport must be at least reasonably represented. Potential discrepancies using a 2-D model combining the effects of chemistry and transport are investigated in Part 2.

[29] Before discussing in a more general sense the influence of stratospheric transport on isotope ratios, we note one additional limitation of the chemistry-only Rayleigh framework presented. The KIEs are temperature dependent, with some of them appreciably larger than others over the range of temperatures in the stratosphere (~180–280 K), such as the hydrogen KIE for CH_4 + Cl. Thus, changes in the absolute and relative magnitudes of the KIEs with stratospheric temperature might also affect observed variations in fractionation factors α^{C}_{strat} and α^{H}_{strat}. Since the temperature dependence of the hydrogen KIEs is stronger than it is for carbon, the effect on the δD-CH_4:CH_4 mixing ratio relationship may be larger than the $\delta^{13}C$-CH_4:CH_4 mixing ratio relationship. However, the observed concavity in Figure 5 occurs for both $\delta^{13}C$-CH_4 and δD-CH_4 and is therefore not likely a direct result of temperature. Nonethe-

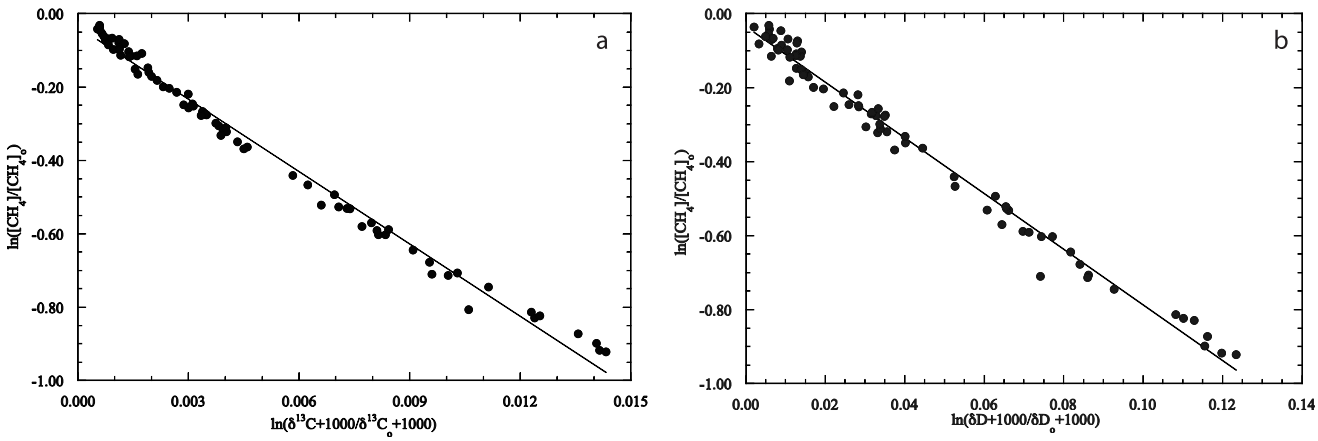

Figure 5. Rayleigh distillation plots for (a) $\delta^{13}C$-CH_4 and (b) δD-CH_4 showing relative change in mixing ratio versus relative change in isotope ratio. Empirically derived average fractionation factors are $\alpha^{C}_{strat} = 1.0154 \pm 0.0008$ (2σ) and $\alpha^{H}_{strat} = 1.153 \pm 0.010$ (2σ).

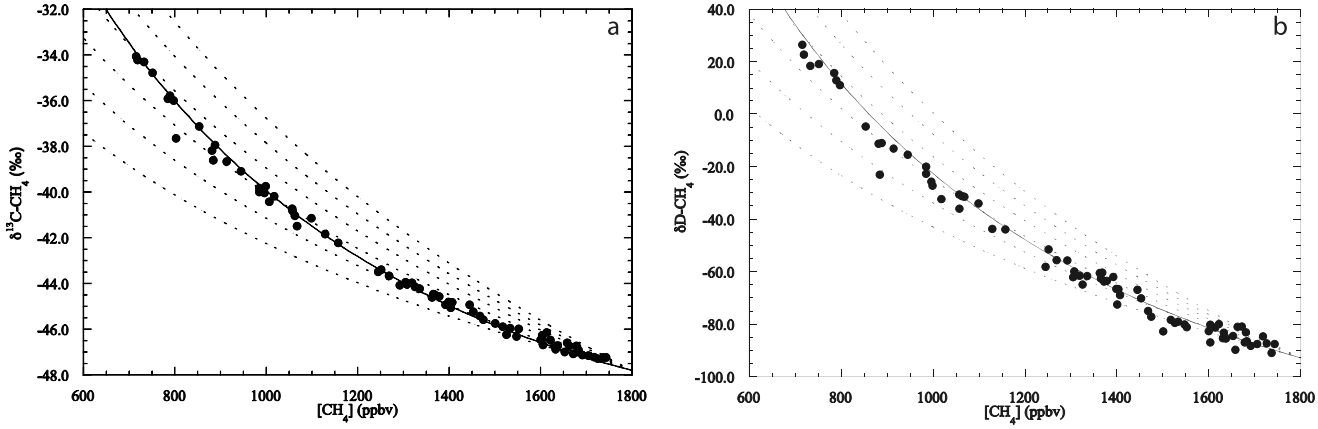

Figure 6. (a) δ^{13}C-CH_4 observations along with Rayleigh curves calculated with constant fractionation factors ranging from 1.010 to 1.020 (dotted lines) and with a monotonically increasing α^{C}_{strat} with respect to decreasing CH_4 mixing ratio (solid lines) from 1.0108 at 1726 ppbv to 1.0204 at 716 ppbv. (b) δD-CH_4 observations along with Rayleigh curves with α ranging from 1.11 to 1.20 (dotted lines) and with a monotonically increasing α^{H}_{strat} with respect to decreasing CH_4 mixing ratio (solid lines) from 1.115 at 1726 ppbv to 1.198 at 716 ppbv.

less, temperature effects cannot be ignored and are explored in the 2-D model study of Part 2.

4.2. Alteration of Chemistry-Only Rayleigh Isotope:Tracer Relationships Due to Transport and Mixing

[30] In general, mixing processes attenuate the heavy isotope enrichment of a species when a given fraction of its initial concentration has been destroyed (i.e., for a given CH_4 mixing ratio in this case). While this can be shown mathematically for a variety of specific mixing processes—such as conservative mixing between two end members or constant input of a gas into a well-mixed box—this effect can be easily understood conceptually. The Rayleigh distillation equation (equation (7)) describes the change in the isotopic composition of chemical species after a given amount of species has been destroyed (i.e., for a given ratio of $[CH_4]/[CH_4]_0$ here). In an isolated, well-mixed system, the fractionation factor, α, is simply given by the kinetic isotope effect (or the weighted-average of the KIEs for CH_4 oxidation as in equation (6), delineated as α_{KIE} for the discussion here). However, suppose that two air parcels with different amounts of CH_4 are mixed together. Even if the isotopic compositions of the CH_4 in each individual air parcel had previously obeyed simple Rayleigh isotope fractionation with a fractionation factor α_{KIE}, the act of mixing these two air parcels together necessarily means that Rayleigh fractionation no longer describes the isotope:CH_4 mixing ratio relationship in the resulting mixture. The mixing of air masses attenuates the isotope fractionation expected from the pure Rayleigh relationship because mixing of an air parcel that has more CH_4 (and therefore a lighter isotopic composition) with an air parcel that has less CH_4 (and therefore a heavier isotopic composition) reduces (i.e., "lightens") the isotopic composition at the resulting CH_4 mixing ratio of the mixture from that which would be predicted simply by the underlying kinetic isotope effect (i.e., by the Rayleigh equation with $\alpha = \alpha_{KIE}$). While it is still possible, though not necessary, that a Rayleigh-type relationship could be used to describe the isotope:tracer relationship in the resulting mixtures of air parcels, the apparent fractionation factor α_{app} (derived from the slope of the $\ln([CH_4]/[CH_4]_0)$:$\ln([1000 + \delta]/[1000 + \delta_0])$ relationship from the mixtures) is necessarily less than α_{KIE}.

[31] For specific application to the stratosphere, note that this reduction in α_{app} from α_{KIE} is true regardless of the type of mixing occurring. The example outlined above might be considered conservative mixing between two air parcels, such as occurs in the lower stratosphere when midlatitude and polar vortex air mix upon break-up of the polar vortex in spring [*Waugh et al.*, 1997; *Herman et al.*, 1998; *Michelsen et al.*, 1999] or due to continuous weak isentropic mixing across the polar vortex edge during the time of maximum descent (and therefore during the time of maximum tracer gradients) [*Plumb et al.*, 2000]. If the stratosphere was a well-mixed box (which, of course, is not the case), the constant input of CH_4 from the troposphere would result in lighter isotope:CH_4 mixing ratio relationships at steady-state than predicted by Rayleigh fractionation, and therefore a smaller α_{app} than that predicted from chemical KIEs alone for the same reason—i.e., the mixing of "high" CH_4 with "low" CH_4 air reduces the fractionation predicted from α_{KIE} for a given CH_4 mixing ratio. Similarly, continuous, weak isentropic mixing across the polar vortex edge during winter [*Plumb et al.*, 2000] would also yield isotope:tracer relationships for which $\alpha_{app} < \alpha_{KIE}$. Although the impact of continuous mixing on the isotope:tracer relationships is mathematically different than that due to conservative mixing, α_{app} is reduced in either case. In general, then, the combination of all mixing processes—such as end-member mixing between polar vortex and midlatitude air, the constant input of CH_4 from the troposphere, as well as finite transport and mixing times between regions of the stratosphere which have different chemical lifetimes for CH_4, for example—all reduce α_{app} below that predicted by α_{KIE}.

[32] Although a specific analysis of which type of mixing is responsible for which possible deviations from a Rayleigh relationship with α_{KIE} is beyond the scope of this

study, the influence of transport on the isotope:tracer relationships is clearly needed to understand the observations. In general, the effect of transport is critical to understand why the apparent carbon and hydrogen fractionation factors, α^{C}_{app} and α^{H}_{app}, derived from the observations are less than the fractionation factors, α^{C}_{KIE} and α^{H}_{KIE}, based on chemistry alone. More specifically, the effect of transport and mixing processes on the isotope: tracer and isotope:isotope relationships are also needed to understand the variations in these relationships with respect to latitude and deployment. The general case has already been discussed extensively. Three examples of these more specific cases are discussed below.

[33] As a first example, mixing and transport explain the small but discernable difference between the $\delta^{13}C$-CH_4:CH_4 mixing ratio relationships in the deep tropics and the extratropics (Figure 4). Air at midlatitudes at 20 km is a mixture of tropical air which has been rapidly transported quasi-horizontally to midlatitudes with older air that has descended from higher altitudes in either the midlatitudes or the polar vortex [e.g., *Andrews et al.*, 2001a]. In contrast, tropical air up to ~20–22 km, while influenced to some degree by isentropic transport from midlatitudes [e.g., *Boering et al.*, 1996; *Volk et al.*, 1996; *Avallone and Prather*, 1997; *Herman et al.*, 1998], is relatively more isolated and has a narrower range of transport histories [e.g., *Andrews et al.*, 1999]. Thus, the observation that $\delta^{13}C$-CH_4 is heavier for a given CH_4 mixing ratio in the tropics than in the extratropics is consistent with the fact that the tropics are comparatively more isolated at ER-2 altitudes than the extratropics. This small difference is not likely to be due to chemistry alone since the in situ chemical lifetimes of CH_4 in both regions are long (>100 years) and approximately equal at ER-2 altitudes. Moreover, model results suggest that if transport is ignored in situ oxidation of CH_4 should produce lighter CH_4 in the tropics based on the oxidant-weighted in situ instantaneous KIEs in those two regions (see Figure 6 of Part 2 [*McCarthy et al.*, 2003]). It should be noted that the difference between the tropics and extratropics in the $\delta^{13}C$-CH_4 data is not observed in the δD-CH_4:CH_4 mixing ratio relationship. This is possibly a consequence of variability observed in this high CH_4 mixing ratio regime being only marginally larger than precision of measurement of δD-CH_4.

[34] As explored further in Part 2, the difference between the $\delta^{13}C$-CH_4:CH_4 mixing ratio relationships in the tropics and extratropics will presumably be much larger at higher altitudes, and, therefore, at lower CH_4 mixing ratios than were obtainable in the tropics with the ER-2. At altitudes above 20–22 km, the tropics are considerably more isolated than at ER-2 altitudes [e.g., *Mote et al.*, 1998]. Thus, the degree of attenuation of α_{KIE} by transport and mixing above 22 km should be even smaller than in the tropical lower stratosphere, which, in turn, implies that the difference between the isotope:tracer relationships in the tropics and extratropics should be even greater at higher altitudes. While low CH_4 whole air samples for high-precision isotope analyses are obtainable from the ER-2 in the extratropics (due to downward transport of air by the stratospheric circulation), low CH_4 samples for isotope analyses in the tropics will have to be collected by balloon or rocket.

[35] A second example of the importance of transport in understanding the ER-2 isotope observations is the difference between the high latitude POLARIS II data points and the high latitude POLARIS I and SOLVE data points for $CH_4 < 1000$ ppbv. The POLARIS II samples were collected in northern summer on 29 and 30 June 1997 while the POLARIS I and SOLVE samples were collected in the Arctic vortex on 26 April 1997 and between 27 January and 12 March 2000, respectively. At 800 ppbv CH_4, $\delta^{13}C$-CH_4 for POLARIS II is almost 2‰ ($\delta^{13}C$) lighter than the POLARIS I and SOLVE vortex data. Although only two samples for POLARIS II were analyzed for $\delta^{13}C$-CH_4 and only one sample for δD-CH_4, these differences are real and not due to measurement or sampling artifacts. This conclusion is based on measurements of both additional WAS samples and simultaneous in situ measurements of N_2O. First, these same samples as well as additional WAS samples from POLARIS II have been analyzed at UC Berkeley for $\delta^{15}N$-N_2O and $\delta^{18}O$-N_2O. Similar to the $\delta^{13}C$-CH_4:CH_4 mixing ratio and δD-CH_4:CH_4 mixing ratio observations, the $\delta^{15}N$-N_2O:N_2O mixing ratio and $\delta^{18}O$-N_2O:N_2O mixing ratio correlations from POLARIS II are also significantly lighter than the SOLVE/POLARIS I vortex data [*Park et al.*, 2002]. Second, the CH_4:N_2O tracer correlations from both the WAS tracer measurements [*Park et al.*, 2002] and the simultaneous in situ CH_4:N_2O tracer correlations [*Herman et al.*, 1998; *Rex et al.*, 1999; *Richard et al.*, 2001] show deviations between the POLARIS II and SOLVE/POLARIS I polar vortex measurements, with the CH_4 mixing ratio for a given N_2O mixing ratio lower in the POLARIS II data for $N_2O < \sim 150$ ppb.

[36] The most likely common reason for these combined deviations in the isotope:tracer and tracer:tracer relationships is due to transport, not chemistry. From satellite, balloon, and aircraft measurements, *Michelsen et al.* [1998], *Herman et al.* [1998] and *Kondo et al.* [1999] have shown that mixing of air that has descended in the vortex with extravortex air reduces the mixing ratio of CH_4 for a given N_2O mixing ratio. This reduction is due to the formation of mixing lines between high and low N_2O air and the fact that the CH_4:N_2O relationship in the extratropics (which represents the initial "prevortex" relationship since the Arctic vortex is formed at the beginning of winter from this air) is nonlinear. An analysis of the CH_4:N_2O correlations from POLARIS I and POLARIS II ER-2 and balloon data sets showed that the vortex data from POLARIS I appeared to be a mixture of high- and low-N_2O air with mixing ratios of ~200 ppb (representative of altitudes of ~20 km) and 25–40 ppb (~32–34 km), respectively, and that the vortex filaments observed during POLARIS II during the summer appeared to be a mixture of 200 ppb air with 15–20 ppb air (~37 km) [*Rex et al.*, 1999]. Thus, CH_4 for a given N_2O mixing ratio is lower for the POLARIS II vortex filaments than for the POLARIS I (as well as SOLVE) vortex samples. For the isotope:tracer relationships, the mixing of these two different "end members" will produce lower isotope values for a given tracer mixing ratio for POLARIS II than for POLARIS I (and SOLVE). Whether this isentropic mixing across the vortex edge occurs throughout the winter ("continuous weak mixing") or after the period of rapid descent (i.e., March or later, dubbed "late end member mixing") is still under

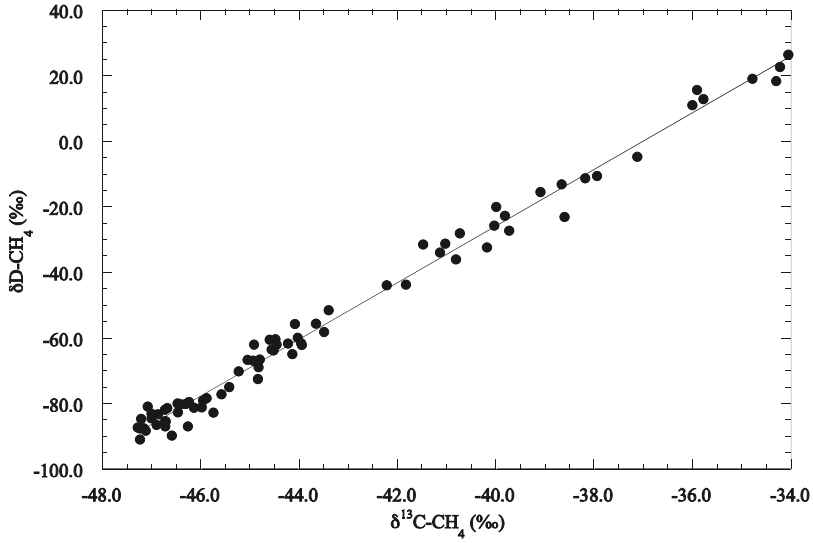

Figure 7. Scatterplot of δD-CH_4 versus δ^{13}C-CH_4.

debate [e.g., *Rex et al.*, 1999; *Plumb et al.*, 2000]. In either case, it is clear that the signature of the "mixed vortex-extravortex" air encountered by the ER-2 in June 1997 at $\theta = 510-530$ K (as well as by a simultaneous balloon flight on 30 June 1997 [*Rex et al.*, 1999]) remained measurable several months after the breakup of the polar vortex due to weak transport at high latitudes in the summer [e.g., *Newman et al.*, 1999]. Thus, the difference in the isotope:tracer relationships at low CH_4 mixing ratios for this particular data set cannot be attributed to a seasonal dependence.

[37] Without these simultaneous N_2O and N_2O isotope measurements, the difference between the POLARIS I and SOLVE vortex data and the summer POLARIS II data might have been interpreted as a signature of ozone hole chemistry in the polar vortex. That is, a heavier δ^{13}C-CH_4:CH_4 mixing ratio relationship in the vortex in spring might result from the large Cl concentrations present in the polar vortex due to heterogeneous processing of $ClONO_2$ and HCl on polar stratospheric clouds [e.g., *Brune et al.*, 1990]. Given that the differences in the isotope:CH_4 mixing ratio relationships measured in samples collected in the polar vortex versus those collected at high latitudes during the summer months can be interpreted as being mainly due to transport alone, the ER-2 CH_4 isotope data of this study do not show direct evidence for such an "activated Cl" effect. Consistent with this interpretation are 2-D model results including heterogeneous chemistry which do not show a change in the isotope:CH_4 mixing ratio relationships due to higher integrated levels of Cl over the course of polar winter [*McCarthy et al.*, 2003]. However, it cannot be ruled out that an activated vortex Cl effect on isotopic compositions would never be discernable; additional data and modeling, particularly for years with little Arctic ozone loss (and correspondingly lower integrated Cl levels) or for the Antarctic vortex (with presumably higher integrated Cl levels), are needed to investigate this potential effect further.

[38] A third example of the importance of the role of transport in determining isotope correlations is the observed compact relationship between δ^{13}C-CH_4 with δD-CH_4 (Figure 7). When considering isotope fractionation produced by chemistry alone, it would be surprising that the significant changes in the fractions of CH_4 oxidized by OH, $O(^1D)$, and Cl as well as significant differences in the carbon versus hydrogen KIEs and their temperature dependences in different regions of the stratosphere would result in a linear relationship between δ^{13}C-CH_4 with δD-CH_4. However, when transport is considered, this high degree of correlation is expected. Considered independently, CH_4, δ^{13}C-CH_4, and δD-CH_4 can all be considered long-lived tracers—that is, their chemical lifetimes are long compared with vertical and horizontal transport timescales. *Plumb and Ko* [1992] have shown that any two tracers that are long-lived with respect to both vertical and horizontal timescales should exhibit a linear correlation (since they are in "slope equilibrium"). The fact that CH_4, δ^{13}C-CH_4, and δD-CH_4 are additionally correlated (since their photochemical production/loss processes are the same, of course) makes this result even less surprising. Nevertheless, transport processes occurring on possibly smaller scales (compared to, e.g., the hemispheric scale), such as mixing across the polar vortex edge, for example, are still discernable in the scatter around the line fit to the observations (e.g., the POLARIS II datum at δ^{13}C-$CH_4 = -38.60$‰).

4.3. Comparison of δ^{13}C-CH_4 Results With Prior Stratospheric Studies

[39] Although measurements from previous studies span different ranges of mixing ratios, a comparison with results reported here is possible by looking at truncated portions of the ER-2 data that span similar ranges in CH_4 mixing ratio. Early measurements reported from the upper troposphere and lower stratosphere in the midlatitude Northern Hemisphere between 12 and 18 km by *Wahlen et al.* [1989] provided an estimate for the carbon stratospheric fractionation factor of $\alpha^C_{strat} = 1.0143 \pm 0.0008$ in samples ranging from 1222 to 1730 pbbv. This value falls between our overall average fractionation factor, $\alpha^C_{strat} = 1.0154 \pm 0.0008$ (2σ), and with our data set truncated at 1220 ppbv to span a similar range of mixing ratios, $\alpha^C_{strat} = 1.0130 \pm 0.0004$ (2σ), and is within the combined uncertainties in either case. However,

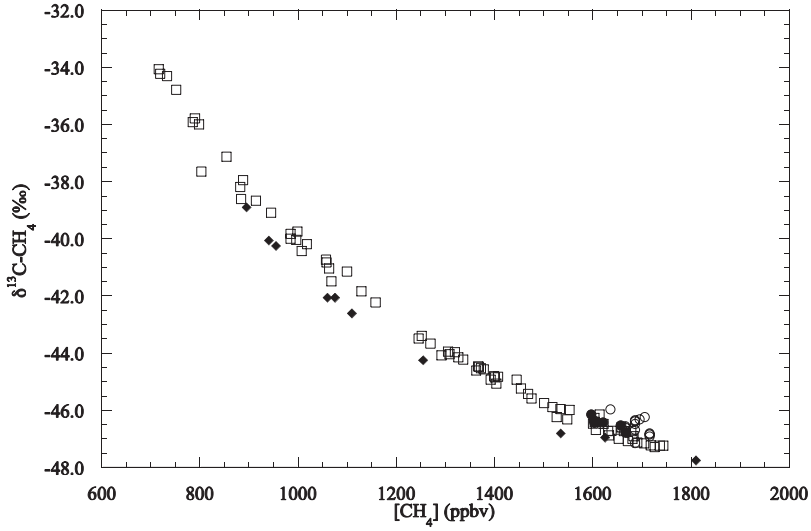

Figure 8. Comparison of δ^{13}C-CH_4 versus CH_4 correlation of ER-2 observations (open squares) with data from *Sugawara et al.* [1997] (diamonds), PEM Tropics A (open circles) [*Tyler et al.*, 1999], AASE II (solid circles) [*Gupta et al.*, 1996].

significant differences in δ^{13}C-CH_4 values reported from the free troposphere (ca. 0.5‰) may reveal interdecadal variations and/or calibration differences that would likely affect a more direct comparison of the δ^{13}C-CH_4:CH_4 mixing ratio relationships. *Brenninkmeijer et al.* [1995] reported measurements of δ^{13}C-CH_4 from large volume (350–600 L) air samples collected in the lower stratosphere (10–12 km) in the middle and high latitude southern hemisphere. Correlation of δ^{13}C-CH_4 and CH_4 mixing ratio of 8 data points with mixing ratio between ~1690 and 1620 ppbv provided a fractionation factor of $\alpha^{C}_{strat} = 1.012$. Their empirically derived value of α^{C}_{strat} is in agreement (likely within uncertainty although none is reported in *Brenninkmeijer et al.* [1995]) with a truncated portion of our data set extending to 1620 ppbv, $\alpha^{C}_{strat} = 1.0110 \pm 0.0004$ (2σ).

[40] A more direct comparison can be made with data from *Sugawara et al.* [1997], the only previous data set to extend well into the stratosphere. They reported 11 measurements from air samples collected over Japan using a balloon-borne cryogenic air sampler. Collection altitudes spanned 14.0 to 34.7 km and mixing ratios spanned 1810 to 895 ppbv. From values of CH_4 mixing ratio and δ^{13}C-CH_4, a stratospheric fractionation factor was calculated to be $\alpha^{C}_{strat} = 1.0131 \pm 0.0006$. This value is within 2σ uncertainty of ER-2 results reported here where the data is truncated so that it does not extend to concentrations lower than 895 ppbv, $\alpha^{C}_{strat} = 1.0142 \pm 0.0005$ (2σ). Despite this apparent agreement, plotting the data side by side in Figure 8 there is a notable offset between the two data sets of greater than ca. 0.5‰ (δ^{13}C) with data from *Sugawara et al.* [1997] isotopically depleted relative to the ER-2 data. This disparity between the data sets is largely removed when the data from *Sugawara et al.* [1997] are arbitrarily adjusted by +1‰ (although this purely empirical adjustment overcorrects for the two data points above 1600 ppbv). This offset may reflect systematic difference between the two laboratories as a result of vacuum line contaminant blank correction procedures (ca. 1.5‰ [*Sugawara et al.*, 1996]) or calibration differences in δ^{13}C-CH_4 and δ^{13}C-CO_2. Although both laboratories are calibrated relative to NIST carbonate isotope standards for $^{13}C/^{12}C$ (UC Irvine is also calibrated against IAEA-CO-9 isotope standard), to date there has been no direct intercomparison of working reference gases between these two laboratories. Additional uncertainty in a comparison of our isotope data to that of *Sugawara et al.* [1997] may arise from differences in IRMS reference gases from scale contraction, a small but significant cross contamination between sample and reference gases in modern differential isotope ratio mass spectrometers [*Allison and Francey*, 1995; *Meijer et al.*, 2000; M. Verkouteren, personal communication, 2002]. The offset may also reflect differences in calibration scales for measurements of CH_4 of mixing ratio, Tohoku University scale compared with NIST scale. Whatever the cause, isotope ratios (δ^{13}C-CH_4) reported in *Sugawara et al.* [1996, 1997] from the well mixed troposphere are in general depleted compared with those reported here and in *Tyler et al.* [1999].

[41] Without a rigorous laboratory intercomparison or additional stratospheric balloon data, it cannot be ruled out that at least some of the ca. 1‰ offset between the balloon and the ER-2 data described above is due to real differences in the air masses sampled (i.e., latitudinal, seasonal, or interannual). However, the relatively tight correlations in isotope:CH_4 mixing ratio relationships observed throughout the mid and high latitudes in these ER-2 data, despite a wide range of altitudes and latitudes sampled, suggest that differences in altitude and latitude of collection alone are not significant factors in determining the isotope value of an air sample. Further, simultaneous balloon and ER-2 measurements have previously shown that tracer:tracer relationships can be very similar on both horizontal and vertical scales [*Herman et al.*, 1998; *Rex et al.*, 1999; *Andrews et al.*, 2001b; *Daube et al.*, 2002]. Thus, it is not unreasonable to expect that the δ^{13}C-CH_4:CH_4 mixing ratio

relationship derived from a balloon profile in the extratropics will be very similar to that derived from ER-2 samples collected below 21 km. Moreover, it is difficult to reconcile how measurements of air samples collected in the midlatitude middle stratosphere could be isotopically depleted when compared with measurements of air from polar vortex remnants which were the result of mixing between (formerly) extratropical air at 37 km and 20 km, since vortex air would be expected to have a depleted isotopic composition for a given mixing ratio. It is also noteworthy that, aside from the 1‰ offset, we observe very little difference between the two data sets in terms of their relationship between $\delta^{13}C$-CH_4 and CH_4 mixing ratio. Therefore it appears the intercalibration explanation is the most likely cause of the offset.

[42] Also shown in Figure 8 is data from the AASE II [*Gupta et al.*, 1996] and PEM Tropics A [*Tyler et al.*, 1999] campaigns, collectively spanning 1600 to 1790 ppbv (originally on the NOAA/CMDL scale but adjusted by 24 ppbv here to be consistent with the NIST scale [e.g., *Gupta et al.*, 1996]). All points but one from the AASE II program are from the mid to high latitude Northern Hemisphere (21 to 73 °N) and were collected between 11 and 13 km altitude [*Gupta et al.*, 1996]; one data point is from the tropical troposphere (8 °S, 11.3 km). The AASE II data are not distinguishable from and fall within the variability of the ER-2 data in the $\delta^{13}C$-CH_4:CH_4 mixing ratio scatterplot of Figure 8. PEM Tropics A measurements are from air samples collected primarily in the extratropical Southern Hemisphere between 3 and 12 km altitudes [*Tyler et al.*, 1999]. In contrast to AASE II data, PEM Tropics A data are isotopically enriched when compared with ER-2 data in Figure 8. As all these previous measurements of $\delta^{13}C$-CH_4 were made at UC Irvine, it is highly unlikely this is a reflection of systematic differences in analyses. Rather, the Southern Hemispheric free troposphere has been characterized to be isotopically enriched relative to the Northern Hemisphere by ~0.1 to 0.5 ‰ ($\delta^{13}C$-CH_4), depending on latitude and time of year [*Quay et al.*, 1999; *Lowe et al.*, 1999]. Differences between PEM Tropics A and ER-2 data can likewise be explained by this interhemispheric gradient.

4.4. Comparison of D/H Results With Prior Stratospheric Studies

[43] There are only two data sets with which to compare these ER-2 measurements of δD-CH_4 in the stratosphere. From measurements of 12 large-volume whole air samples collected from the upper troposphere and lower stratosphere, *Wahlen et al.* [1989] estimated an average fractionation factor of $\alpha^{H}_{strat} = 1.129 \pm 0.021$ over the concentration range 1319 to 1730 ppbv. With the ER-2 data set truncated at 1320 ppbv to span a similar range in CH_4 mixing ratios, a value of $\alpha^{H}_{strat} = 1.131 \pm 0.006$ (2σ) is obtained. The results agree within 1σ error bars with those of *Wahlen et al.* [1989]. As noted in comparison of $\delta^{13}C$-CH_4 data, however, it is unclear how these data directly compare since dissimilarity between these two data sets may arise from calibration differences and decadal scale variations. Results may also be compared with values derived from analyses of high resolution solar occultation infrared spectra from the Atmospheric Trace Molecule Spectroscopy (ATMOS) Fourier-transform interferometer on board the Space Shuttle [*Irion et al.*, 1996]. These spectroscopic measurements of CH_4 and CH_3D in the stratosphere range from altitudes of 15 to 28 km and have a vertical resolution of 2 km. From a fit of the correlation between CH_3D and CH_4 an average fractionation factor for the mid and lower stratosphere was derived: $\alpha^{H}_{strat} = 1.19 \pm 0.02$ (1σ). This value of α^{H}_{strat} is similar to the one derived from the ER-2 data for CH_4 mixing ratios below 1200 ppbv, $\alpha^{H}_{strat} = 1.173 \pm 0.010$ (2σ). The large variability in δD-CH_4 values from the ATMOS measurements (>100‰), however, are not present in the ER-2 data set, consistent with the low precision of the spectroscopic measurements (estimated to be ±74 ‰ (1σ) combined with systematic errors due to large errors for spectroscopic isotope measurements and low spatial resolution) rather than representing real atmospheric variability.

5. Conclusions

[44] These new CH_4 isotope measurements on whole air samples collected aboard the NASA ER-2 aircraft during the STRAT, POLARIS, and SOLVE campaigns comprise the most extensive, high-precision data set for stratospheric $\delta^{13}C$-CH_4 and δD-CH_4 reported to date. Observations over a wide range of latitudes, altitudes, and seasons provide the first accounting of general trends and variability in these isotopic species in the lower stratosphere. We find that a combination of chemistry and transport determines the isotope:tracer relationships observed, with underlying chemical kinetic isotope effects associated with CH_4 sink reactions enriching CH_4 in the heavy isotopes (^{13}C and deuterium) as CH_4 is oxidized in the stratosphere.

[45] Specifically, the ER-2 data clearly show the limitations of the Rayleigh (chemistry-only) model to stratospheric CH_4 observations over large ranges of mixing ratio where multiple sink processes act on CH_4 in changing proportions in different regions of the stratosphere. Nonlinearity in Figure 5 (Rayleigh plot) illustrates our finding that observed fractionation factors increase systematically as CH_4 mixing ratios decrease in the stratosphere. Thus, when comparing empirically derived fractionation factors from different data sets, a meaningful comparison can only be made over comparable ranges in CH_4 mixing ratio. Over the entire range of stratospheric CH_4 mixing ratios observed in this data set (1725 to 716 ppbv) α^{C}_{strat} varies from 1.0108 ± 0.0004 to 1.0204 ± 0.0004 and α^{H}_{strat} varies from 1.115 ± 0.008 to 1.198 ± 0.008.

[46] Scatterplots of these two isotopomer tracers with CH_4 mixing ratio provide fairly tight correlations. Even so, small differences in the $\delta^{13}C$-CH_4:CH_4 mixing ratio relationships with respect to latitude were observed. The deep tropical (<10°N) lower stratosphere observations are heavier in $\delta^{13}C$-CH_4 for a given CH_4 mixing ratio than those in the extratropics, although the difference is small and near the precision of the measurements. Tropical-extratropical differences are expected to be larger at lower CH_4 mixing ratios than were observable from the ER-2 samples collected in the tropics—i.e., at altitudes >21 km.

[47] Differences in the isotope:CH_4 mixing ratio measurements at low CH_4 mixing ratios (<1000 ppb) for the samples collected during POLARIS II in the summer and the samples collected in the Arctic vortex during the

POLARIS I and SOLVE deployments are due to transport and not to elevated Cl levels from heterogeneous processing of $ClONO_2$ and HCl in the vortex. This conclusion is based on the correlation of both WAS and in situ CH_4 and N_2O mixing ratios as well as isotope measurements on the same samples for $\delta^{15}N$ and $\delta^{18}O$ of N_2O.

[48] Measurements from this study represent a new set of "double constraints" for CH_4 chemical oxidative processes in the stratosphere (i.e., for integrated OH, Cl, and $O(^1D)$ oxidation) combined with transport. Here in Part 1, we compared observed fractionation factors with those expected based on a chemistry-only model and derived lower bounds for the amount of CH_4 oxidation by the Cl and $O(^1D)$ channels at both high and low CH_4 mixing ratios. For the $\delta^{13}C$-CH_4 data, reasonable fractions of f_{Cl} were obtained but are clearly only lower bounds since attenuation of the observed isotope fractionation due to transport was not accounted for. For the δD-CH_4 data, ignoring transport led to unrealistically high bounds for $f_{O(^1D)}$, likely due to the fact that the hydrogen KIE with OH is much larger than that for the carbon case; thus transport will play a more critical role in attenuation of fractionation effects than for $\delta^{13}C$-CH_4. In Part 2, we compare predictions of the isotope:tracer relationships from a 2-D model with the observations and examine the sensitivity of the predictions to uncertainties and discrepancies in experimentally determined carbon and hydrogen KIEs. Uncertainties in the hydrogen and carbon KIEs, as well as in modeled stratospheric OH, Cl, and $O(^1D)$ levels and transport, all play a role in our ability to reproduce the observations. Ultimately, however, the double set of constraints provided here should serve — in an iterative process of new modeling and experimental studies and comparisons with observations — to reduce uncertainties in CH_4 isotope fractionation in the atmosphere. Decreasing the uncertainties in the KIEs and furthering our quantitative understanding of CH_4 isotope fractionation in the stratosphere will not only aid stratospheric studies but will also decrease uncertainties in using the isotopic composition of CH_4 in the troposphere to better quantify the CH_4 budget.

[49] **Acknowledgments.** We thank Stephen Donnelly, Rich Lueb, and Sue Schauffler for expert collection of samples used in this study, and Verity Stroud for methane mixing ratio analyses. Additional thanks go to Michael Bender of Princeton University for measurements of $\delta^{15}N$-N_2 and to Sunyoung Park for analysis of and insight into the N_2O isotope and CH_4:N_2O data mentioned. We have appreciated the advice of Ralph Cicerone and thank him for his valuable discussions. Research support at NCAR was provided from the NASA Upper Atmosphere Program and the National Science Foundation. The National Center for Atmospheric Research is operated by the University Corporation for Atmospheric Research under the sponsorship of the National Science Foundation. Research support for UC Berkeley was provided by the NSF Atmospheric Chemistry Program (ATM-9901463), the NASA Upper Atmosphere Research Program (NAG 2-1483), and a Packard Foundation Fellowship for KAB. Research support for UC Irvine was provided by a major research instrumentation award from NSF (ATM-9871077), a research grant from NASA (NAG5-9955), and a NASA Earth System Science Fellowship (NAGTA5-50226) for AR.

References

Allison, C. E., and R. J. Francey, High precision stable isotope measurements of atmospheric trace gases, in *Reference and Intercomparison Materials for Stable Isotopes of Light Elements*, *IAEA TECDOC-825*, p. 153, Int. At. Energy Agency, Vienna, Austria, 1995.

Andrews, A. E., K. A. Boering, B. C. Daube, S. C. Wofsy, E. J. Hintsa, E. M. Weinstock, and T. P. Bui, Empirical age spectra for the lower tropical stratosphere from in situ observations of CO_2: Implications for stratospheric transport, *J. Geophys. Res.*, *104*(D21), 26,581–26,595, 1999.

Andrews, A. E., K. A. Boering, S. C. Wofsy, B. C. Daube, D. B. Jones, S. Alex, M. Loewenstein, J. R. Podolske, and S. E. Strahan, Empirical age spectra for the midlatitude lower stratosphere from in situ observations of CO_2: Quantitative evidence for a subtropical "barrier" to horizontal transport, *J. Geophys. Res.*, *106*(D23), 10,257–10,274, 2001a.

Andrews, A. E., et al., Mean ages of stratospheric air derived from in situ observations of CO_2, CH_4, and N_2O, *J. Geophys. Res.*, *106*(D23), 32,295–32,314, 2001b.

Avallone, L. M., and M. J. Prather, Tracer-tracer correlations: Three-dimensional model simulations and comparisons to observations, *J. Geophys. Res.*, *102*(D15), 19,233–19,246, 1997.

Bergamaschi, P., C. Brühl, C. A. M. Brenninkmeijer, G. Saueressig, J. N. Crowley, J. U. Grooß, H. Fischer, and P. J. Crutzen, Implications of the large carbon kinetic isotope effect in the reaction CH_4 + Cl for the $^{13}C/^{12}C$ ratio of stratospheric CH_4, *Geophys. Res. Lett.*, *23*, 2227–2230, 1996.

Bergamaschi, P., M. Braunlich, T. Marik, and C. A. M. Brenninkmeijer, Measurements of the carbon and hydrogen isotopes of atmospheric methane at Izana, Tenerife: Seasonal cycles and synoptic-scale variations, *J. Geophys. Res.*, *105*(D11), 14,531–14,546, 2000.

Blake, D. R., and F. S. Rowland, Continuing worldwide increase in tropospheric methane, 1978 to 1987, *Science*, *239*, 1129–1131, 1988.

Boering, K. A., S. C. Wofsy, B. C. Daube, H. R. Schneider, M. Loewenstein, and J. R. Podolske, Stratospheric mean ages and transport rates from observations of carbon dioxide and nitrous oxide, *Science*, *274*, 1340–1343, 1996.

Boone, G. D., F. Agyin, D. J. Robichaud, F. M. Tao, and S. A. Hewitt, Rate constants for the reactions of chlorine atoms with deuterated methanes: Experiment and theory, *J. Phys. Chem. A*, *105*(9), 1456–1464, 2001.

Brenninkmeijer, C. A. M., D. C. Lowe, M. R. Manning, R. J. Sparks, and P. F. J. Vanvelthoven, The ^{13}C, ^{14}C, and ^{18}O isotopic composition of CO, CH^4, and CO^2 in the higher southern latitudes lower stratosphere, *J. Geophys. Res.*, *100*(D12), 26,163–26,172, 1995.

Brune, W. H., D. W. Toohey, J. G. Anderson, and K. R. Chan, In situ observations of ClO in the Arctic stratosphere—ER-2 aircraft results from 59-degrees-N to 80-degrees-N latitude, *Geophys. Res. Lett.*, *17*(4), 505–508, 1990.

Cantrell, C. A., R. E. Shetter, A. H. McDaniel, J. G. Calvert, J. A. Davidson, D. C. Lowe, S. C. Tyler, R. J. Cicerone, and J. P. Greenberg, Carbon kinetic isotope effect in the oxidation of methane by the hydroxyl radical, *J. Geophys. Res.*, *95*(D13), 22,455–22,462, 1990.

Coplen, T. B., Reporting stable carbon, hydrogen, and oxygen isotopic abundances, in *Reference and Intercomparison Materials for Stable Isotopes of Light Elements*, *IAEA TECDOC-825*, p. 31, Int. At. Energy Agency, Vienna, Austria, 1995.

Coy, L., E. R. Nash, and P. A. Newman, Meteorology of the polar vortex: Spring 1997, *Geophys. Res. Lett.*, *24*(22), 2693–2696, 1997.

Craig, H., Isotopic standards for carbon and oxygen and correction factors for mass-spectrometric analysis of carbon dioxide, *Geochim. Cosmochim. Acta*, *12*, 133–149, 1957.

Craig, H., and C. C. Chou, Methane: The record in polar ice cores, *Geophys. Res. Lett.*, *9*, 1221–1224, 1982.

Crowley, J. N., G. Saueressig, P. Bergamaschi, H. Fischer, and G. W. Harris, Carbon kinetic isotope effect in the reaction CH_4 + Cl: A relative rate study using FTIR spectroscopy, *Chem. Phys. Lett.*, *303*(3–4), 268–274, 1999.

Crutzen, P. J., Role of the tropics in atmospheric chemistry, in *The Geophysiology of Amazonia*, edited by R. E. Dickinson, pp. 107–130, John Wiley, New York, 1987.

Daube, B. C., K. A. Boering, A. E. Andrews, and S. C. Wofsy, A high-precision fast-response CO_2 analyzer for in situ sampling from the surface to the middle stratosphere, *J. Atmos. Oceanic Technol.*, *19*, 1532–1543, 2002.

Davidson, J. A., C. A. Cantrell, S. C. Tyler, R. E. Shetter, R. J. Cicerone, and J. G. Calvert, Carbon kinetic isotope effect in the reaction of CH_4 with HO, *J. Geophys. Res.*, *92*, 2195–2199, 1987.

DeMore, W. B., Rate constant ratio for the reactions of OH with CH_3D and CH_4, *J. Phys. Chem.*, *97*(33), 8564–8566, 1993.

Denning, R. F., S. L. Guidero, G. S. Parks, and B. L. Gary, Instrument description of the Airborne Microwave Temperature Profiler, *J. Geophys. Res.*, *94*, 16,757–16,765, 1989.

Dickinson, R. E., and R. J. Cicerone, Future global warming from atmospheric trace gases, *Nature*, *319*, 109–115, 1986.

Dlugokencky, E. J., B. P. Walter, K. A. Masarie, P. M. Lang, and E. S. Kasischke, Measurements of an anomalous global methane increase during 1998, *Geophys. Res. Lett.*, *28*(3), 499–502, 2001.

Donner, L., and V. Ramanathan, Methane and nitrous oxide: Their effects on the terrestrial climate, *J. Atmos. Sci.*, *37*, 119–124, 1980.

Etheridge, D. M., G. I. Pearman, and P. J. Fraser, Changes in tropospheric methane between 1841 and 1978 from a high accumulation-rate antarctic ice core, *Tellus, Ser. B*, *44*(4), 282–294, 1992.

Etheridge, D. M., L. P. Steele, R. J. Francey, and R. L. Langenfelds, Atmospheric methane between 1000 AD and present: Evidence of anthropogenic emissions and climatic variability, *J. Geophys. Res.*, *103*(D13), 15,979–15,993, 1998.

Flocke, F., et al., An examination of chemistry and transport processes in the tropical lower stratosphere using observations of long-lived and short-lived compounds obtained during STRAT and POLARIS, *J. Geophys. Res.*, *104*(D21), 26,625–26,642, 1999.

Gierczak, T., R. K. Talukdar, S. C. Herndon, G. L. Vaghjiani, and A. R. Ravishankara, Rate coefficients for the reactions of hydroxyl radicals with methane and deuterated methanes, *J. Phys. Chem. A*, *101*(17), 3125–3134, 1997.

Gonfiantini, R., W. Stichler, and K. Rozanski, Standards and intercomparison materials distributed by the international atomic energy agency for stable isotope measurements, in *Reference and Intercomparison Materials for Light Elements*, *IAEA TECDOC-825*, p. 13, Int. At. Energy Agency, Vienna, Austria, 1995.

Greenblatt, J. B., et al., Defining the polar vortex edge from an N_2O:potential temperature correlation, *J. Geophys. Res.*, *107*(D20), 8268, doi:10.1029/2001JD000575, 2002.

Gupta, M., S. Tyler, and R. Cicerone, Modeling atmospheric $\delta^{13}C$-CH_4 and the causes of recent changes in atmospheric CH_4 amounts, *J. Geophys. Res.*, *101*(D17), 22,923–22,932, 1996.

Herman, R. L., et al., Tropical entrainment timescales inferred from stratospheric N_2O and CH_4 observations, *Geophys. Res. Lett.*, *25*(15), 2781–2784, 1998.

Hoefs, J., *Stable Isotope Geochemistry*, Springer-Verlag, New York, 1987.

Irion, F. W., et al., Stratospheric observations of CH_3D and HDO from atmospheric infrared solar spectra—Enrichments of deuterium in methane and implications for HD, *Geophys. Res. Lett.*, *23*(17), 2381–2384, 1996.

Kaye, J. A., Mechanisms and observations for isotopic fractionation of molecular species in planetary atmospheres, *Rev. Geophys.*, *25*, 1609–1658, 1987.

Kondo, Y., et al., NO_y-N_2O correlation observed inside the Arctic vortex in February 1997: Dynamical and chemical effects, *J. Geophys. Res.*, *104*(D7), 8215–8224, 1999.

Levy, H., Normal atmosphere: Large radical and formaldehyde concentrations predicted, *Science*, *17*(3), 141–143, 1971.

Lowe, D. C., et al., Shipboard determinations of the distribution of ^{13}C in atmospheric methane in the Pacific, *J. Geophys. Res.*, *104*(D21), 26,125–26,135, 1999.

McCarthy, M. C., P. Connell, and K. A. Boering, Isotopic fractionation of methane in the stratosphere and its effect on free tropospheric isotopic compositions, *Geophys. Res. Lett.*, *28*(19), 2657–2660, 2001.

McCarthy, M. C., K. A. Boering, A. L. Rice, S. C. Tyler, P. Connell, and E. Atlas, Carbon and hydrogen isotopic compositions of stratospheric methane: 2. Two-dimensional model results and implications for kinetic isotope effects, *J. Geophys. Res.*, *108*, doi:10.1029/2002JD003183, in press, 2003.

Meijer, H. A. J., R. E. M. Neubert, and G. H. Visser, Cross contamination in dual inlet isotope ratio mass spectrometers, *Int. J. Mass Spectrom.*, *198*, 45–61, 2000.

Michelsen, H. A., G. L. Manney, M. R. Gunson, C. P. Rinsland, and R. Zander, Correlations of stratospheric abundances of CH_4 and N_2O derived from ATMOS measurements, *Geophys. Res. Lett.*, *25*(15), 2777–2780, 1998.

Michelsen, H. A., et al., Intercomparison of ATMOS, SAGE II, and ER-2 observations in Arctic vortex and extra-vortex air masses during spring 1993, *Geophys. Res. Lett.*, *26*(3), 291–294, 1999.

Mote, P. W., T. J. Dunkerton, M. E. McIntyre, E. A. Ray, P. H. Haynes, and J. M. Russell, Vertical velocity, vertical diffusion, and dilution by midlatitude air in the tropical lower stratosphere, *J. Geophys. Res.*, *103*(D8), 8651–8666, 1998.

Newman, P. A., D. W. Fahey, W. H. Brune, and M. J. Kurylo, Including special sections—Photochemistry of Ozone Loss in the Arctic Region in Summer (POLARIS) CACGP/IGAC 1998 Symposium (CACGP/IGAC)—Preface, *J. Geophys. Res.*, *104*(D21), 26,481–26,496, 1999.

Newman, P., et al., An overview of the SOLVE-THESEO 2000 campaign, *J. Geophys. Res.*, *107*(D20), 8259, doi:10.1029/2001JD001303, 2002.

Park, J. H., E. Atlas, and K. A. Boering, Observations of the fractionation of nitrous oxide isotopomers in the stratosphere, *Eos Trans. AGU*, *83*(19), Spring Meet. Suppl., B31A-04, 2002.

Plumb, R. A., and M. K. W. Ko, Interrelationships between mixing ratios of long-lived stratospheric constituents, *J. Geophys. Res.*, *97*(D9), 10,145–10,156, 1992.

Plumb, R. A., D. W. Waugh, and M. P. Chipperfield, The effects of mixing on traces relationships in the polar vortices, *J. Geophys. Res.*, *105*(D8), 10,047–10,062, 2000.

Quay, P., J. Stutsman, D. Wilbur, A. Snover, E. Dlugokencky, and T. Brown, The isotopic composition of atmospheric methane, *Global Biogeochem. Cycles*, *13*(2), 445–461, 1999.

Ramanathan, V., R. J. Cicerone, H. B. Singh, and J. T. Kiehl, Trace gas trends and their potential role in climate change, *J. Geophys. Res.*, *90*, 5547–5566, 1985.

Ramaswamy, R., O. Boucher, J. Haigh, D. Hauglustaine, J. Haywood, G. Myhre, T. Nakajima, G. Y. Shi, and S. Solomon, Radiative forcing of climate change, in *Climate Change 2001: The Scientific Basis, Contribution of Working Group I to the Third Assesment Report of the Intergovernmental Panel on Climate Change*, pp. 350–416, Cambridge Univ. Press, New York, 2001.

Rasmussen, R. A., and M. A. K. Khalil, Atmospheric methane in the recent and ancient atmospheres: Concentrations, trends, and interhemispheric gradient, *J. Geophys. Res.*, *89*, 11,599–11,605, 1984.

Rex, M., et al., Subsidence, mixing, and denitrification of Arctic polar vortex air measured during POLARIS, *J. Geophys. Res.*, *104*, 26,611–26,623, 1999.

Rice, A. L., A. A. Gotoh, H. O. Ajie, and S. C. Tyler, High-precision continuous-flow measurement of $\delta^{13}C$ and δD of atmospheric CH_4, *Anal. Chem.*, *73*(17), 4104–4110, 2001.

Richard, E. C., et al., Severe chemical ozone loss inside the Arctic Polar Vortex during winter 1999–2000 inferred from in situ airborne measurements, *Geophys. Res. Lett*, *28*(11), 2197–2200, 2001, (Corrigendum, *Geophys. Res. Lett.*, *28*(16), 3167–3168, 2001.).

Robbins, R. C., L. A. Cavanagh, L. J. Salas, and E. Robinson, Analysis of ancient atmospheres, *J. Geophys. Res.*, *78*, 5341–5344, 1973.

Saueressig, G., P. Bergamaschi, J. N. Crowley, H. Fischer, and G. W. Harris, Carbon kinetic isotope effect in the reaction of CH_4 with Cl atoms, *Geophys. Res. Lett.*, *22*(10), 1225–1228, 1995.

Saueressig, G., P. Bergamaschi, J. N. Crowley, H. Fischer, and G. W. Harris, D/H kinetic isotope effect in the reaction CH_4 + Cl, *Geophys. Res. Lett.*, *23*(24), 3619–3622, 1996.

Saueressig, G., J. N. Crowley, P. Bergamaschi, C. Bruhl, C. A. M. Brenninkmeijer, and H. Fischer, Carbon 13 and D kinetic isotope effects in the reactions of CH_4 with $O(^1D)$ and OH: New laboratory measurements and their implications for the isotopic composition of stratospheric methane, *J. Geophys. Res.*, *106*(19), 23,127–23,138, 2001.

Scott, S. G., T. P. Bui, K. R. Chan, and S. W. Bowen, The meteorological measurement system on the NASA ER-2 aircraft, *J. Atmos. Oceanic Technol.*, *7*, 525–540, 1990.

Shine, K. P., Y. Fouquart, V. Ramaswamy, S. Solomon, and J. Srinivasan, Radiative forcing of climate change, in *Climate Change 1995: The Science of Climate Change, Scientific Assessment Work Group I of Intergovernmental Panel on Climate Change*, pp. 108–118, Cambridge Univ. Press, New York, 1996.

Steele, L. P., P. J. Fraser, R. A. Rasmussen, M. A. K. Khalil, T. J. Conway, A. J. Crawford, R. H. Gammon, K. A. Masarie, and K. W. Thoning, The global distribution of methane in the troposphere, *J. Atmos. Chem.*, *5*, 125–171, 1987.

Stevens, C. M., and F. E. Rust, The carbon isotopic composition of atmospheric methane, *J. Geophys. Res.*, *87*(14), 4879–4882, 1982.

Stichler, W., Interlaboratory comparison of new materials for carbon and oxygen isotope ratio measurements, in *Reference and Intercomparison Materials for Stable Isotopes of Light Elements*, *IAEA TECDOC-825*, p. 153, Int. At. Energy Agency, Vienna, Austria, 1995.

Sugawara, S., T. Nakazawa, G. Inoue, T. Machida, H. Mukai, N. Vinnichenko, and U. Khattatov, Aircraft measurements of the stable carbon isotopic ratio of atmospheric methane over Siberia, *Global Biogeochem. Cycles*, *10*(2), 223–231, 1996.

Sugawara, S., T. Nakazawa, Y. Shirakawa, K. Kawamura, S. Aoki, T. Machida, and H. Honda, Vertical profile of the carbon isotopic ratio of stratospheric methane over Japan, *Geophys. Res. Lett.*, *24*(23), 2989–2992, 1997.

Thompson, A. M., and R. J. Cicerone, Possible perturbations to atmospheric CO, CH_4, and OH, *J. Geophys. Res.*, *91*, 10,853–10,864, 1986.

Tyler, S. C., H. O. Ajie, M. L. Gupta, R. J. Cicerone, D. R. Blake, and E. J. Dlugokencky, Stable carbon isotopic composition of atmospheric

methane: A comparison of surface level and free tropospheric air, *J. Geophys. Res.*, *104*(D11), 13,895–13,910, 1999.

Tyler, S. C., H. O. Ajie, A. L. Rice, R. J. Cicerone, and E. C. Tuazon, Experimentally determined kinetic isotope effects in the reaction of CH_4 with Cl: Implications for atmospheric CH_4, *Geophys. Res. Lett.*, *27*(12), 1715–1718, 2000.

Volk, C. M., et al., Quantifying transport between the tropical and mid-latitude lower stratosphere, *Science*, *272*, 1763–1768, 1996.

Wahlen, M., B. Deck, R. Henry, A. Shemesh, R. Fairbanks, W. Broecker, H. Weyer, B. Marino, and J. Logan, Profiles of $\delta^{13}C$ and δD of CH_4 from the lower stratosphere, *Eos Trans. AGU*, *70*, 1017, 1989.

Wang, J., M. McElroy, C. Spivakovsky, and D. B. A. Jones, On the contribution of anthropogenic Cl to the increase in (13C of atmospheric methane, *Global Biogeochem. Cycles*, *16*(3), 1047, doi:10.1029/2001GB001572, 2002.

Waugh, D. W., et al., Mixing of polar vortex air into middle latitudes as revealed by tracer-tracer scatterplots, *J. Geophys. Res.*, *102*(D11), 13,119–13,134, 1997.

E. Atlas, Atmospheric Chemistry Division, National Center for Atmospheric Research, Boulder, CO 80305, USA.

K. A. Boering and M. C. McCarthy, Department of Chemistry, University of California, Berkeley, CA 94720, USA.

A. L. Rice, Joint Institute for the Study of the Atmosphere and Ocean, University of Washington, Seattle, WA 98195-5351, USA. (arice@ocean.washington.edu)

S. C. Tyler, Department of Earth System Science, University of California, Irvine, CA 92717, USA.